

High Throughput Analysis of microRNA Regulation of MGAT3

by

Fatema Tuz Zohora

A thesis submitted in partial fulfillment of the requirements for the degree of

Master of Science

Department of Chemistry

University of Alberta

© Fatema Tuz Zohora, 2023

## Abstract

Studies related to miRNAs and their ability to alter protein expression have gained much attention in recent years. miRNAs are short single stranded non-coding RNAs (~20 nts) that function in RNA silencing and post-transcriptional modification of gene expression. These short non-coding RNAs primarily bind to the 3'-untranslated region (UTR) of target mRNA transcript. This interaction can cause either translational repression or inhibition mainly via mRNA degradation. miRNAs can also bind to the 5'-untranslated region of target mRNA and regulate protein expression in humans, though the general role of 5'-untranslated region in miRNA mediated regulation still remains unknown.

In the field of glycobiology, miRNAs are now given special consideration as they now have been proven to be a key regulator in many glycosylation pathways. *N*-linked branching of glycans is one of the important glycosylation pathways in eukaryotes and is critical for both the structural and functional integrity of many eukaryotic proteins. Several glycosyltransferase enzymes mainly encoded by MGAT genes are involved in the synthetic pathway of *N*-linked branching. MGAT3 ( $\beta$ -1,4-mannosyl-glycoprotein 4-beta-N-acetylglucosaminyltransferase) enzyme is responsible for the addition of a bisecting GlcNAc to the core mannose residue of complex or hybrid *N*-glycans. The addition of bisecting GlcNAc is a unique modification of complex *N*-glycans that has been reported to play important role in

signal transduction and growth factor signaling pathway, tumor progression and metastasis.

In this thesis, we aim to generate a comprehensive map of the regulation of MGAT3 by miRNA using a newly developed high throughput assay: miRFluR. This assay uses a genetically encoded dual-color fluorescence reporter to identify regulatory miRNA-mRNA interactions. At first we cloned 3'UTR sequence of MGAT3 into empty pFmiR backbone downstream to cerulean protein. Then we co-transfected this 3'UTR-plasmid sensor of MGAT3 with a library of 2601 miRNAs that represent the known human miRNAome in HEK293T cells. After 48 hours of transfection, we performed a ratiometric analysis of cerulean and mCherry protein expression and established a complete map of miRNAs regulating MGAT3 protein expression.

miRFluR assay data revealed a significant number of miRNAs upregulating MGAT3 expression as opposed to their common repression mechanism. These up-regulatory miRNAs were later validated in three different mammalian cancer cell lines by Western blot, RT-qPCR, PHA-E lectin staining and site specific mutation of 3'UTR-sequence of MGAT3. Total 125 up-regulatory miRNAs were identified from the assay compare to only 15 down-regulatory miRNAs. This indicates the dominance of miRNA-mediated upregulation over MGAT3. In addition to that the up-regulatory miRs are highly enriched in cancer pathways predicting the potential role of MGAT3 in cancer. miRNA regulation of genes has been shown to predict functional roles in disease pathways. Thus mapping MGAT3 has enabled us to look deep into the functions of MGAT3 and bisecting GlcNAc in diseases.

## Preface

**Chapter 1** contains a brief introduction to miRNAs, their discovery, biogenesis, mechanism of gene regulation, significance of glycosylation and role of MGAT3 and bisecting GlcNAc in N-linked branching pathway. **Figure 1-3.** is adapted with permission from Reily, C., Stewart, T.J., Renfrow, M.B. et al. Glycosylation in health and disease. *Nat Rev Nephrol* **15**, 346–366 (2019). Copyright © Nature Publishing Group. All other figures were created with BioRender.com© **Chapter 2** contains methodology and experimental workflow and data analysis process of miRFluR assay. Materials and methods used in for miRFluR assay and validation experiments have also been discussed. In **Chapter 3** results of miRFluR assay and data analysis as well as data from post-assay validation experiments have been discussed. Chapter 3 contains non-published work. **Chapter 4** contains a conclusion discussing the overall summary of the thesis. I conducted all the experiments and performed data analysis.

## **Acknowledgments**

Pursuing this degree for me came with its own unique challenges. There are many people I need to thank for making this possible. First, I would like to thank my supervisor Professor Dr. Lara K Mahal for her wonderful guidance and constant support throughout my journey. Apart from being a great scientist and mentor, she is also a kind human being that I always hope to be. I also like to thank my colleagues, my fellow lab mates who have become a lifetime of friends in my life. Special thanks to Helia, Faezeh, Thu, Tigist, Dawn for always being there for me.

My journey would not have become possible without the constant support and motivation from my family and friends living in Bangladesh. I am truly grateful to all of them for always loving me, taking care of me in my thick and thin. I want to thank my husband for the kind of support he provided me for the last few months. I still don't know how I would have survived without him. Thank you so much for your love and support.

And lastly, I like to thank and remember my late parents Mohammad Belayet Hossain and Entezer Begum. I cannot explain in words how much I miss them. I pray to Almighty Allah to comfort my parents' departed souls and for giving me strength to become the person they always wanted me to become and fulfill my parents' dream.

## Table of Contents

Abstract.....	ii
Preface .....	iv
Acknowledgments.....	v
Table of Contents.....	vi
List of Tables .....	viii
List of Figures.....	ix
<b>Chapter 1: Introduction .....</b>	<b>1</b>
<b>1.1. An Overview of MicroRNAs .....</b>	<b>1</b>
1.1.1. miRNA Biogenesis.....	2
1.1.2. miRNA-mediated gene regulation mechanism .....	4
1.1.3. Predicting miRNA target and gene regulatory network .....	6
1.1.4. High-throughput miRFluR assay for the identification of miRNA-target interactome .....	8
<b>1.2. An introduction to Glycans and their significance.....</b>	<b>10</b>
1.2.1 Structural diversity of glycans .....	11
1.2.2. N-linked glycosylation and role of bisecting GlcNAc.....	13
<b>1.3. Significance of miRNAs in the study of glycosylation .....</b>	<b>17</b>
<b>1.4. Overview of thesis .....</b>	<b>19</b>
<b>Chapter 2: Methodology.....</b>	<b>21</b>
<b>2.1. Experimental design and workflow .....</b>	<b>21</b>
<b>2.2. Materials and methods .....</b>	<b>25</b>
2.2.1. Cloning.....	25
2.2.2. Cell culture .....	26
2.2.3. miRFluR assay.....	26
2.2.4. Western blot .....	28
2.2.5. RT-qPCR .....	30
2.2.6. PHA-E lectin staining .....	30
2.2.7. Site directed mutagenesis .....	31
<b>Chapter 3: Results and Discussion .....</b>	<b>34</b>
<b>3.1. MGAT3 is predominantly upregulated by miRNAs in miRFluR assay.....</b>	<b>34</b>
<b>3.2. Selection of miRNAs for post-assay validation experiments .....</b>	<b>36</b>

<b>3.3. Western Blot validation in mammalian cancer cell lines.....</b>	<b>38</b>
<b>3.4. RT-qPCR data in HT29 and A549 cell line.....</b>	<b>43</b>
<b>3.5. PHA-E lectin staining detects bisecting GlcNAc level follows miRFluR assay.....</b>	<b>46</b>
<b>3.6. Site specific mutation of 3'UTR sequence revealed miR-92a-1 5p directly binds to MGAT3 – 3'UTR and mediate upregulation .....</b>	<b>48</b>
<b>Chapter 4: Conclusion .....</b>	<b>51</b>
<b>References.....</b>	<b>54</b>
<b>Appendix-1. 3'UTR sequence of MGAT3.....</b>	<b>61</b>
<b>Appendix-2. MGAT3-3' UTR mutated sequence.....</b>	<b>62</b>
<b>Appendix-3. PHA-E lectin staining in A549 cell line .....</b>	<b>63</b>
<b>Appendix-4. PHA-E lectin staining in HT29 .....</b>	<b>64</b>
<b>Appendix-5: List of miRNA hits for MGAT3 in the miRFluR assay .....</b>	<b>65</b>
<b>Appendix-6: Ponceau images of Western blots in HT29 .....</b>	<b>68</b>
<b>Appendix-7: Ponceau images of Western blots in A549 .....</b>	<b>70</b>
<b>Appendix-8: Ponceau images of Western Blots in PANC1.....</b>	<b>71</b>

## List of Tables

<b>Table-1.</b> Primer list for cloning pmiR-MGAT3-3'UTR sensor .....	25
<b>Table-2.</b> Primer list for RT-qPCR.....	29
<b>Table-3.</b> List of primers for cloning mutated pmiR-3'UTR sensor.....	32
<b>Table-4.</b> Selected miRNA hit list of MGAT3 for post-assay validation experiments.....	36
<b>Appendix-5.</b> List of miRNA hits for MGAT3 in the miRFluR assay.....	62

## List of Figures

<b>Figure 1-1.</b> An illustration of canonical and non-canonical miRNA biogenesis pathways.....	3
<b>Figure 1-2.</b> miRNA mediated gene repression mechanism.....	4
<b>Figure 1-3.</b> Schematic representation of high-throughput miRFluR assay.....	9
<b>Figure 1-4.</b> Major components of human glycome.....	11
<b>Figure 1-5.</b> Biosynthetic pathway of N-linked glycosylation in ER and Golgi.....	13
<b>Figure 1-6.</b> Enzymes involved in N-linked glycosylation and synthesis of bisecting GlcNAc.....	14
<b>Figure 1-7.</b> Effect of miRNA in altering MGAT3 protein expression.....	18
<b>Figure 2-1.</b> Plasmid map for pmiR-3'UTR sequence of MGAT3.....	22
<b>Figure 2-2.</b> Experimental workflow of miRFluR assay.....	23
<b>Figure 2-3.</b> Schematic representation of site specific mutation experiment of pFmiR-3' UTR sensor.....	32
<b>Figure 3-1.</b> miRFluR assay data analysis.....	34
<b>Figure 3-2.</b> Western Blot validation data in HT29.....	38
<b>Figure 3-3.</b> Western Blot validation data in PANC1.....	39
<b>Figure 3-4.</b> Western Blot validation data in A549.....	40
<b>Figure 3-5.</b> Western blot validation data for anti-miRs. ....	41
<b>Figure 3-6.</b> RT-qPCR data in HT29 cell line.....	43
<b>Figure 3-7.</b> RT-qPCR data in A549 cell line.....	44
<b>Figure 3-8.</b> PHA-E lectin staining of HT29 cells. ....	46
<b>Figure 3-9.</b> PHA-E lectin staining of A549 cells.....	47
<b>Figure 3-10.</b> Site specific mutation analysis for miR-92a-1-5p.....	49
<b>Appendix 3.</b> PHA-E lectin staining in A549 cell line.....	63
<b>Appendix 4.</b> PHA-E lectin staining in HT29.....	64
<b>Appendix-6.</b> Ponceau images of Western blots in HT29.....	68
<b>Appendix-7.</b> Ponceau images of Western blots in A549.....	70
<b>Appendix-8.</b> Ponceau images of Western Blots in PANC1.....	71

## Chapter 1: Introduction

### 1.1. An Overview of MicroRNAs

microRNAs (miRNAs) are small non-coding RNAs (ncRNAs), typically of 19 to 24 nucleotides in length that act as post-transcriptional regulators of gene expression. miRNAs were first discovered in 1993 when a group of scientists discovered the regulatory effect of a tiny RNA encoded by the *lin-4* gene on the *lin-14* protein in *Caenorhabditis elegans* nematodes. Downregulation of *lin-14* protein is essential for the progression of the larval stage of these organisms and was found to be directly dependent on a *lin-4* in the initial transition. Transition from the late larval stage to the adult stage required another small RNA named *let-7*. Surprisingly, these small RNAs did not translate into biologically active proteins. Later it was found that both of these RNAs had complementary sequences in the 3' untranslated region (UTR) of their target mRNAs resulting in a downregulation of the gene expression.<sup>1,2,3</sup>

Soon after this discovery, homologs of *let-7* were discovered in the genome of human and flies. Additionally, *let-7* RNA was found in human, *Drosophila*, and eleven other bilateral species.<sup>3</sup> These small non-coding RNAs were later termed microRNAs. Since their discovery, they have been found in almost all eukaryotes and select miRNAs are conserved across various species.<sup>3</sup> To date, 2,654 mature miRNA sequences have been annotated in the human genome.<sup>4</sup> Discovery of new miRNAs is ongoing. It is now well-established that miRNAs play a vital role in critical cellular functions at the post-transcriptional level. By binding primarily at the 3'- untranslated region (UTR) of target mRNA, they can finely tune the expression of a target gene and alter protein level.<sup>5</sup> miRNAs play a more significant role in regulating gene expression

networks by targeting multiple genes that are functionally related. Therefore, changes in the expression of a single miRNA can have a broad impact on the expression of many genes and the overall function of the cell or organism. Although studies related to miRNA biogenesis and their regulatory mechanism in humans are well documented, recent studies have shown more complex pathways involved in miRNA-mediated gene regulation. The following sections briefly review miRNA biogenesis, regulatory mechanism, and their association with disease pathways.

### **1.1.1. miRNA biogenesis**

miRNA encoding sequences are located in the exons or introns of either protein coding genes or intergenic regions. They can be co-regulated together by their host genes or can be under control of their own promoters. Genes that produce miRNA are usually transcribed by RNA polymerase II or III to form primary miRNA (pri-miRNAs) which can be up to several thousand nucleotides and shaped as hairpin structures.<sup>6</sup> These pri-miRNAs then go onto a multistep process to become mature miRNAs following either the canonical or non-canonical biogenesis pathways **(Figure 1-1)**.

In the canonical pathway, Drosha, an RNase III family member, in complex with DGCR8 digests the primary miRNA (pri-miRNA) hairpin into precursor miRNA (pre-miRNA). In contrast, the non-canonical pathway generates pre-miRNAs via mRNA splicing machinery, bypassing the need for Drosha-DGCR8 mediated digestion in the nucleus. In either pathway, pre-miRNAs are transported to the cytoplasm by the nuclear export protein Exportin 5 and then further processed by

a second RNase III enzyme, Dicer and TARBP (TAR-RNA binding protein 2). The mature double-stranded miRNAs are then loaded onto the RNA-induced silencing complex (RISC), a ribonucleoprotein complex responsible for miRNA-mediated post-transcriptional gene silencing. RISC comprises multiple protein factors, with Argonaute (AGO) proteins serving as the key catalytic enzymes within the complex. AGO proteins bind miRNAs and are crucial for downstream gene-regulatory mechanisms that regulate mRNA degradation and protein expression.<sup>7,8</sup>

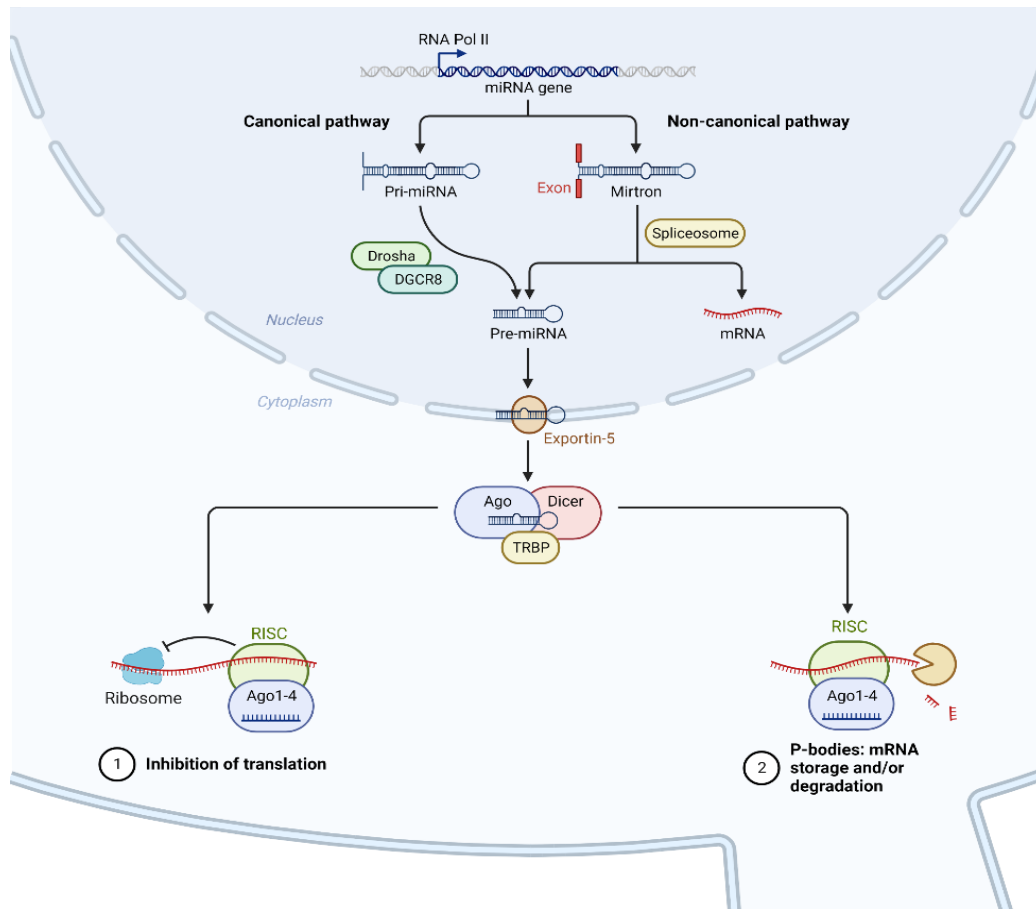


**Figure 1-1:** An illustration of canonical and non-canonical miRNA biogenesis pathways.

### 1.1.2. miRNA-mediated gene regulation mechanism

Putative knowledge of regulation by miRNA revolves around their ability to alter protein levels by downregulation. Currently, there are 3 commonly accepted mechanisms for miRNA action- i) Translational repression by inhibiting translation initiation, ii) Post-initiation translational repression by impeding the elongation of polysome, leading to ribosomal stalling, and iii) miRNA-mediated decapping and/or deadenylation. (Figure 1-2).

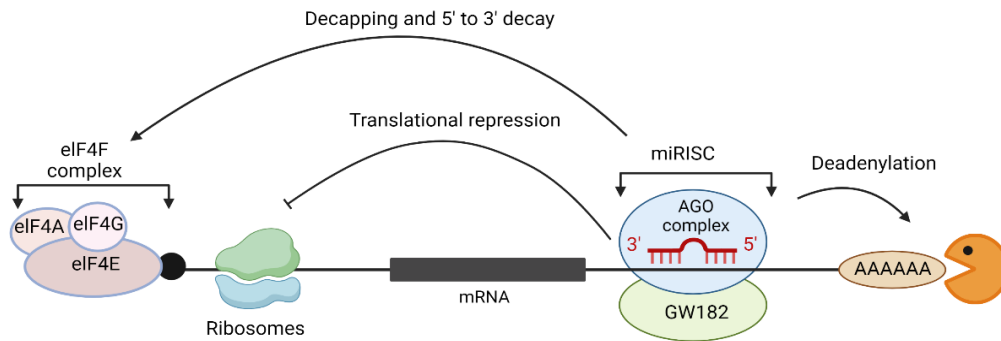


**Figure 1-2: miRNA mediated gene repression mechanism.** Three most commonly assumed gene repression mechanisms for miRNAs are presented here. miRNA induced silencing complex (miRISC) is composed ribonucleoproteins (miRNPs). AGO1-4 complex is essential for miRNA mediated regulation of gene while GW182 has been reported to bind with AGO complex for miRNA mediated silencing.

In the pre-translational initiation phase, miRNA-mediated silencing complexes (miRISCs) act by affecting eukaryotic translation initiation factor 4F (eIF4F) cap recognition causing 5' to 3' decay of target mRNA. In post-initiation translational repression, miRISCs can inhibit polysome elongation, preventing the ribosome from moving along the mRNA molecule and resulting in stalling of the ribosome. It causes them to drop off the mRNAs or facilitates the degradation of newly synthesized peptides.<sup>9</sup> miRISCs can also destabilize target mRNAs by binding to them and recruiting RNA decapping enzymes (DCP1/2) and/or deadenylating enzymes complexes, leading to mRNA degradation.<sup>10</sup> P-bodies play a critical role in the storage and degradation of targeted mRNAs. P-bodies are rich in enzymes and protein complexes that can affect the translational machinery by mRNA degradation and sequestration. One of the known P-body components GW182, also known as TNRC6, has been found to physically interact with AGO proteins in the miRISC complex during the miRNA-mediated gene repression process.<sup>11</sup> When miRISCs bind to target mRNAs, they can be transported into P-bodies for storage, but may re-enter the translation phase under certain circumstances like stress.<sup>12</sup>

Emerging evidence suggests that miRNAs possess a broad range of regulatory mechanisms, extending beyond their established role in translational repression. In contrast to the general assumption of miRNA-mediated downregulation, studies have reported that miRNA can also upregulate target gene expression in a particular cellular state (e.g., quiescent cells, mitochondrial cells) depending on the presence of specific co-factors such as shortened poly-A tail or destabilized mRNA.<sup>13,14,15</sup> However, a more

recent study on miRNA-mRNA interaction from our lab has found evidence of miRNA upregulation of protein expression in actively dividing cancer cells. Although the underlying mechanism of miRNA mediated upregulation is still unknown, our study revealed the possible association of Fragile X mental retardation syndrome-related protein 1(FXR1) with AGO2 instead of GW182 in the upregulation process.<sup>16</sup> These findings give insight into the multifaceted nature of miRNA's role and function for gene regulation. It is still unclear how and when a particular mechanism prevails in a particular condition, which miRNA-mRNA binding rules correspond to each mechanism, and which factors are crucial in regulating these mechanisms. More research is necessary to gain a better understanding of how miRNAs work and their effects.

### **1.1.3. Predicting miRNA target and gene regulatory network**

miRNAs and their ability to target gene expression have gained much attention in recent years. More and more studies have been carried out to identify potential miRNA targets. While early studies on miRNAs often focused on individual miRNA-target interactions and their effects on specific pathways, it is now widely recognized that miRNAs act as key regulators of gene expression networks. Each miRNA typically targets multiple genes, and many of these genes are functionally related, meaning that they are involved in the same biological pathways or processes. As a result, changes in the expression of a single target gene can have far-reaching effects on the overall regulatory network and functioning of the cell or organism. This complexity has led to a growing interest in systems-level approaches to studying miRNA-target network

analysis, which can help to identify the key biological processes and pathways that are regulated by that particular network.

However, establishing a complete targetome and gene regulatory network for miRNAs is still a major challenge. Our knowledge about potential targets of miRNAs mostly come from miRNA target prediction algorithms which heavily rely on the canonical rules of “seed” pairing, i.e., the perfect consecutive base-pairing between the target mRNA and the miRNA in the seed region, which typically involves positions 2-7 or 2-8 at the 5' end of miRNA.<sup>17</sup> This pattern has been verified through crystallographic studies of ribonucleoprotein AGO-miRNA complexes.<sup>18</sup> Although the seed region is important for target silencing, it is not the only determinant of miRNA-mRNA interaction. For example, G:U wobble base pairs are often tolerated within the seed region, and extensive base-pairing at the 3' end of the miRNA may offset missing complementarity at the seed region.<sup>19,20</sup> Additionally, centered sites, exhibiting 11-12 contiguous base-pairing in the central region of the miRNA without pairing to either end, have also been reported.<sup>21</sup> Moreover, some studies have reported efficient silencing from sites that do not conform to any of the aforementioned patterns, appearing random. Furthermore, sites with extensive 5' complementarity may not always exhibit activity when tested in reporter constructs.<sup>22,23</sup> The complex nature of miRNA-mRNA interactions is the prime reason for the poor prediction accuracy of prediction algorithms. Tools like TargetScan, miRANDA, miRWALK etc. incorporate factors such as binding site accessibility, AU rich elements, evolutionary conservation in addition to seed pairing but still show poor prediction result with an accuracy rate of only 20-60%.<sup>24,25</sup> This underscores the importance of an experimental approach for

identifying miRNA targets. However, miRNAs are growing in number and the experimentally validated miRNA-target interaction numbers are comparatively low.<sup>26</sup> Current high-throughput experimental approaches for miRNA target validation are based on transcriptomic analysis and crosslinking immunoprecipitation assays (CLIP). However, both of these methods do not always correspond to the regulatory changes that take place on protein level. This is more significant for low abundance genes, like glycogenes, where relying solely on transcriptomic data may result in inaccuracies due to the intrinsic noise present in the data. Fluorescent reporter assays are currently used as standard methods for identifying miRNA-target interactions. However, they are low to moderate throughput in nature allowing investigation of only a single miRNA at a time. Recently, our lab has developed a high-throughput, genetically encoded dual color fluorescence reporter based system- miRFluR to map miRNA-target interaction for the entire miRome. It has allowed us to map the interaction between a target gene and an entire cohort of miRNAs in the biological system at a single time; bringing more of an “omics” approach to the study of miRNA mediated gene regulation.<sup>5</sup>

#### **1.1.4. High-throughput miRFluR assay for the identification of miRNA-target interactome**

The identification of miRNA:target interactomes faces significant challenges in modern research. There is a low accuracy and sensitivity in predicting these interactions, with success rates ranging between 17-66%.<sup>7</sup> Existing reporter assays such as the luciferase assay, provide more accurate results but they are not highly scalable. High-throughput transcriptomic profiling is not the ideal method for comprehending

the protein regulatory network of miRNAs. This is much more significant for lower gene expression levels, particularly for glycogenes that present technical complications in both transcriptomic analysis and RISC complex pulldown.

To develop a better high-throughput platform and create an accurate miRNA-target database based on validated miRNA-target interactions, our lab has recently introduced miRFluR assay. The assay utilizes a genetically encoded fluorescent ratiometric reporter to identify miRNA-target 3'UTR interactions in 384 well plates<sup>5</sup> (**Figure 1-3**). The miRFluR assay uses pFmiR-3'UTR plasmid sensor to identify regulatory miRNA-target interactions. miRNAs primarily bind to the 3'UTR region of the target gene. That is why the system requires 3'UTR sequence of a gene of interest cloned downstream of cerulean, the primary reporter protein. The sensor contains a second fluorescent protein, mCherry, acting as a control. This sensor is then co-transfected with a miRNA mimic library (2601 miRNAs) into HEK293t cells aliquoted in 384 well-plates. 48 hours post-transfection, the data are analyzed for ratiometric cerulean/mCherry expression levels. The data are normalized to the ratios for a non-targeting control (NTC) miRNA that is present in all plates. If the miRNA represses the target gene then the cerulean/mCherry ratio will be lower than the NTC. If the ratio is higher, then the miRNA is upregulating the target gene.

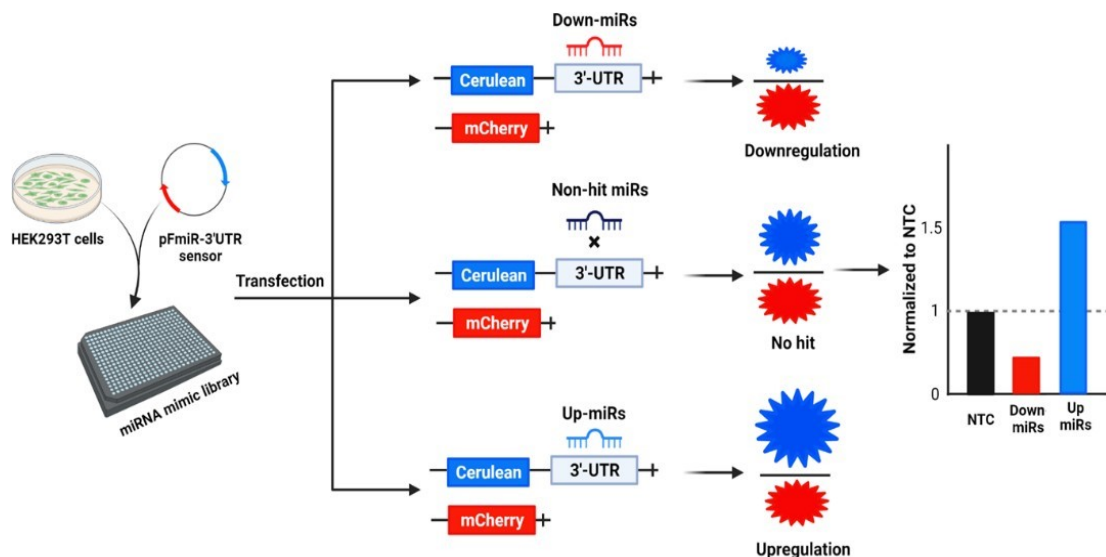


**Figure 1-3:** Schematic representation of high-throughput miRFluR assay.

miRFluR assay surpasses the limitation of all the challenges we faced before to established miRNA-target interactome. With the increasing amount of information about genuine miRNA-target interactions, we will be better equipped to utilize this data to gain a better understanding of the biological roles played by miRNAs and their target genes.

## 1.2. An introduction to glycans and their significance

Glycans are long-chained carbohydrates and are one of the most abundant macromolecules that decorate almost every cell in human body. Along with nucleic acids, proteins, and lipids, glycans are one of the four fundamental classes of molecules that make up all living systems. They play a crucial role in various aspects of cell and organismal biology, including cell adhesion, molecular trafficking and clearance, receptor activation, signal transduction and endocytosis.<sup>27</sup> The glycocalyx, a thick layer

of glycans covering the cell surface, can protrude more than 30 nm from the plasma membrane in some cells, consequently surrounding cell surface proteins by a matrix of glycans.<sup>28</sup> Glycosylation is an intricate biological process, governed by hundreds of glycosylation enzymes catalyzing the transfer of activated forms of monosaccharides (building blocks of glycan) from a donor molecule to an acceptor molecule i.e., protein or lipid. It is the most abundant and diverse post-translational modification process which has enormous capacity to alter biological function in different disease conditions. To date more than 130 rare genetic or metabolic disorders have been identified due to any defect in complex glycosylation process.<sup>29</sup>

### **1.2.1 Structural diversity of glycans**

Glycans in nature are often conjugated. Most protein and lipid molecules in different cellular compartments are covalently attached to glycans making them structurally diverse and complex in nature. More than 200 glycosylation enzymes are reported to drive the glycosylation process through which glycans are synthesized, altered or attached to a polypeptide or lipid backbone. There are nine monosaccharide residues most commonly found in mammals that act as building blocks of glycan structure.<sup>30</sup>

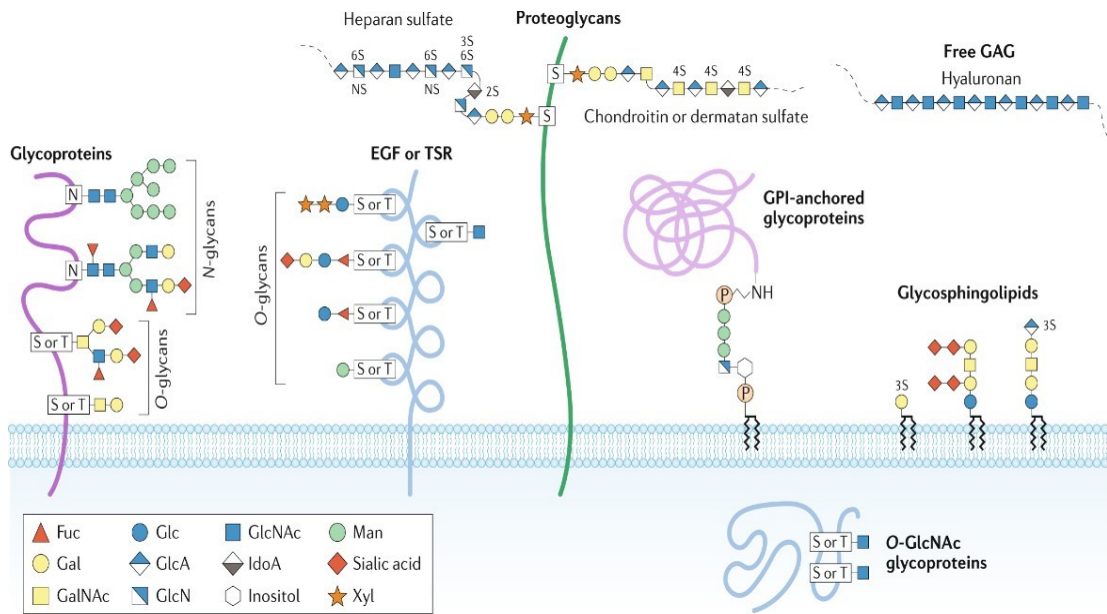


**Figure 1-4: Major components of human glycome.** Glycan structures present here represent the most common forms of cellular glycome components in human. This illustration has been adapted with permission from Reily, C., et al.<sup>31</sup>, Nature Review of Nephrology.

Glycosylation takes place predominantly in the secretory pathway of the cell. More specifically, the biosynthetic process of glycans starts at the endoplasmic reticulum (ER) and then move to Golgi apparatus where they become highly oligomeric and branched as they transit to the cell surface or other extracellular compartments.<sup>32</sup> Protein glycosylation mostly represents N-glycans, O-glycans and proteoglycans (also known as glycosaminoglycans). N-glycans are linked to the amide group of asparagine residues of proteins often in a consensus with Asn-X-Ser/Thr motif. O-linked glycans

are characterized by their bond to the hydroxyl group of the serine and threonine residues in proteins. Proteoglycans are also linked to the serine or threonine motifs but they are linear in structure, follows a different biosynthetic pathway than O-linked glycans and are highly sulfated. Glycosylphosphatidylinositol (GPI)-anchored proteins are another modification where the GPI-linked proteins are found in the lipid bilayer facing the extracellular compartment. Lipid glycosylation is also prevalent in secretory pathway that produce in glycosphingolipid. In addition to this, hyaluronan is a unique glycan type that is unattached to any protein or lipid and secreted into extracellular compartments.<sup>27,33</sup>

### **1.2.2. N-linked glycosylation and role of bisecting GlcNAc**

N-linked glycosylation is one of the most diverse and structurally complex glycosylation modifications that takes place in ER and Golgi complex. It is evident that N-linked glycans undergo significant modifications as they move through the ER and the Golgi complex, eventually reaching their final destinations within or outside the cell. During early stages of protein synthesis, when the variety of oligosaccharide structures is limited, these glycans play a crucial role in protein folding, oligomerization, quality control, sorting, and transportation processes.<sup>34</sup>

Biosynthesis of N-linked glycosylation generally has three major steps. The first one is the synthesis of dolichol-phosphate (Dol-P) linked precursor that comprises of N-acetylglucosamine (GlcNAc), glucose and mannose residues. This single precursor N-glycan is then transferred to a nascent glycoprotein in the second step and undergoes trimming of glucose and mannose residues from the precursor structure. The

final step involves the branching and core modification of mature N-glycans to produce hybrid and complex structures. This late processing of mature N-glycans starts at the medial Golgi and regulated by glycosyl transferase enzymes primarily encoded by MGAT genes. Biosynthesis of complex N-glycans initiated in the medial-Golgi compartment yields a bi-antennary structure which can lead to the tri and tetra antennary structures of complex N-glycans (**Figure 1-5 and 1-6**). Complex and hybrid structures can sometimes have an additional sugar residue called "bisecting" GlcNAc. This residue is attached to the  $\beta$ -Man sugar of the core structure by an enzyme called  $\beta$ -1,4-mannosyl-glycoprotein 4- $\beta$ -N-acetylglucosaminyltransferase (MGAT3).

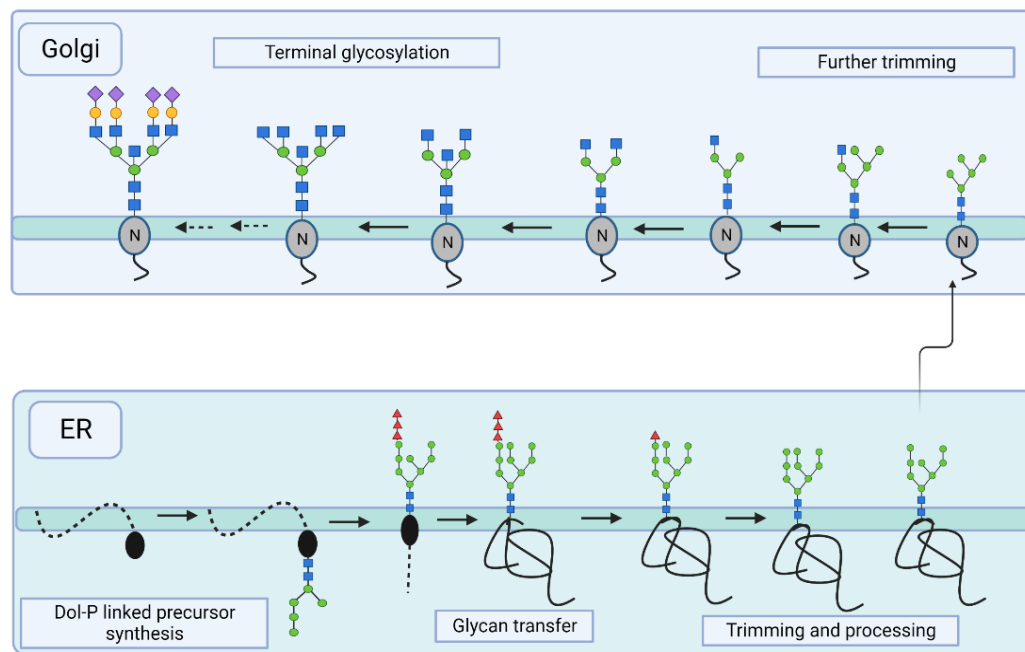


**Figure 1-5: Biosynthetic pathway of N-linked glycosylation in ER and Golgi.** An illustration of biosynthetic pathway of N-linked glycosylation. The process starts with the synthesis dolichol-phosphate (Dol-P) linked precursor synthesis in endoplasmic

reticulum. The synthesis of terminal hybrid and complex N-glycans take place in Golgi. Glycan symbols are drawn according to Symbol Nomenclature for Glycans (SNFG) format.

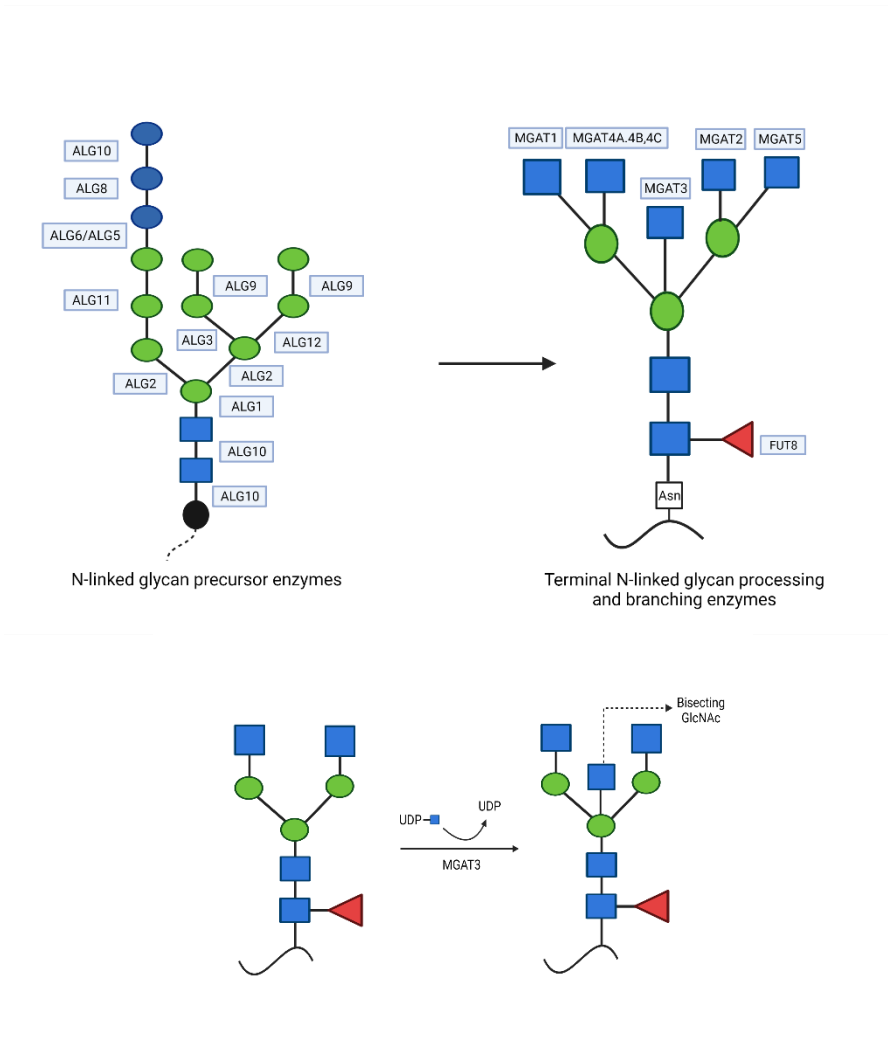


**Figure 1-6: Enzymes involved in N-linked glycosylation and synthesis of bisecting GlcNAc.** N-linked glycosylation enzymes can be classified into two groups. Dol-P linked precursor synthesis enzymes are predominantly present in ER and terminal N-linked glycan processing and branching enzymes are present in cis, trans and medial

Golgi. Addition of bisecting GlcNAc to core mannose residue of bi-antennary N-glycan structure is catalyzed by MGAT3 enzyme. UDP-GlcNAc acts as the substrate. Glycan symbols are drawn according to Symbol Nomenclature for Glycans (SNFG) format.

The addition of bisecting GlcNAc to the core mannose residue of hybrid or complex N-glycans is a unique modification that plays important role in various biological processes. It can affect cell adhesion, fetal development, signal transduction, growth factor signaling, neurogenesis, tumor metastasis and development, and immune biology.<sup>35</sup> For example, altered levels of bisecting GlcNAc on integrin  $\beta 1$  have been linked to early spontaneous miscarriages in humans, while its presence on glycoproteins has been found to inhibit hypoxia-induced epithelial-mesenchymal transition in breast cancer cells.<sup>36,37</sup> Additionally, increased levels of glycoproteins with bisecting GlcNAc have been reported in ovarian carcinoma and glioblastoma leading to a poor prognosis and survival rate.<sup>38</sup> The presence of bisecting GlcNAc on glycoproteins can also confer resistance to natural killer cells. In addition to their roles in disease prognosis, bisecting GlcNAc can also play crucial role in tuning N-glycan branching by preventing further branching and elongation for hybrid N-glycans. Addition of bisecting GlcNAc restricts the activity of MGAT5 and FUT8 enzymes, responsible for initiating branching and core-fucosylation in complex N-glycans respectively. In cancer cells, N-glycans tend to become more branched, which promotes the progression of cancer. Thus MGAT3 may play a crucial role as a tumor suppressor in select cancerous cells.<sup>39</sup> On the contrary, aberrant synthesis of bisecting GlcNAc can also alter the cellular and molecular function of N-glycans, leading to

impaired immunity, neuronal cell migration, emphysema, or inflammation.<sup>35</sup> Given the importance of MGAT3 and subsequent bisecting GlcNAc synthesis, it is crucial to further investigate its functions and implications.

### **1.3. Significance of miRNAs in the study of glycosylation**

Changes in glycosylation can change inflammatory responses, promote viral immune escape, cancer cell metastasis or regulate apoptosis.<sup>31</sup> Abnormal glycosylation has been identified as a characteristic feature of cancer, playing a significant role in the development and progression of the disease. Many of the tumor biomarkers currently used in clinical practice are glycoproteins,<sup>40</sup> which shows the importance of investigating the underlying mechanisms of aberrant glycosylation and translating these findings into clinical applications. However, glycosylation is a complex regulatory network that requires hundreds of glycosyltransferase and glycosidase enzymes to coordinate in an intricate manner. Genes encoding glycosylation enzymes are very low in abundance, making it difficult to study their regulation at the transcriptomic level, leading to a poor understanding of corresponding regulatory mechanism in a particular biological process.

miRNAs have emerged as critical regulators of the cellular glycome in recent years. Our lab has previously established miRNAs as major regulators of glycogenes.<sup>41</sup> In previous work from our lab, we saw several glycogenes being targeted by miRNA-200 family and phenocopying their biological effect on epithelial to mesenchymal transition (EMT) and cell migration.<sup>42</sup> This finding was extremely significant and led to the miRNA proxy hypothesis which states, “If a miR drives a specific biological

phenotype, such as migration or metastasis, the targets of that miR will drive the same biological phenotype.”<sup>5</sup> But to test the hypothesis and see glycosylation enzymes truly imitate the concordant miRNA effect, it was necessary to identify and validate miRNAs targeting glycogenes in biological condition. This led to the development of high throughput miRFluR assay from our lab to map a complete miRNA regulatory network for a particular glycogene in a high throughput manner. To date, our lab has established miRNA-glycogene regulatory network for three glycogenes- B3GLCT, ST6GAL1 and ST6GAL2 leveraging miRFluR assay.<sup>5,16</sup> According to the miRNA prediction algorithms, B3GLCT was primarily thought to be highly regulated by miRNAs. However, miRFluR assay revealed <4% of predicted miRNAs targeting the gene with more than 96% false positive rate. In addition to that both down-regulatory and up-regulatory miRNAs were identified for B3GLCT and validated at the protein and mRNA levels. Enrichment analysis of miRNA hits also identified Peters’ Plus syndrome, the known disorder caused by mutation of B3GLCT gene supporting miRNA-proxy hypothesis.<sup>5</sup> Similar to B3GLCT, miRFluR analysis of ST6GAL1 and ST6GAL2 also identified significant numbers of up-regulatory miRNAs. ST6GAL1 was predominantly regulated by up-regulatory miRNAs where ST6GAL2 was mostly downregulated. A subset of miRNA hits were validated in mammalian cancer cell lines. In contrast to the dominant view of miRNA mediated down regulation, high-throughput analysis of ST6GAL1 and ST6GAL2 revealed that up-regulatory interactions may be more conventional than anticipated.<sup>16</sup>

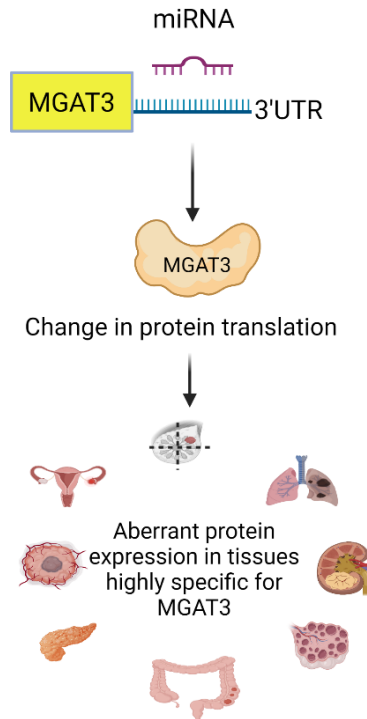


**Figure 1-7: Effect of miRNA in altering MGAT3 protein expression.** Upon binding to 3'UTR of MGAT3, miRNA can alter the protein expression in specific tissue leading to disease pathogenesis.

#### 1.4. Overview of thesis

The aim of this thesis is to generate a comprehensive map of the miRNA-MGAT3 regulatory network using the newly developed high throughput miRFluR assay. MGAT3 is responsible for the addition of bisecting GlcNAc to N-glycan structure that holds an unprecedented role in disease pathways and tuning of N-glycan branching. But the majority of the functional role of MGAT3 is still unknown to the researchers. Since miRNAs are critical regulators of human glycome, mapping the

miRNA-MGAT3 regulatory network for the entire cohort of human miRNAs will give us substantial insight into the regulatory function of MGAT3 in a high throughput manner.

In this thesis, we start with an overview of miRNAs and glycosylation highlighting the significance of MGAT3 and bisecting GlcNAc in disease pathogenesis. Then we present methodology describing the experimental design and workflow of the project. The framework of the project can be divided into three parts i.e., cloning of pmiR-3'UTR plasmid sensor for MGAT3, running miRFluR assay and validation of the assay by western blot, qPCR, PHA-E lectin staining and site directed mutagenesis experiments. The results and data analysis are discussed in the next chapter followed by a conclusion.

## Chapter 2: Methodology

### 2.1. Experimental design and workflow

The experimental design of the thesis has three major components- i) cloning of pmiR-3'UTR plasmid sensor for MGAT3, ii) mapping miRNA-target interaction on high throughput miRFluR assay platform and iii) conducting validation assays to test miRFluR assay data.

The miRFluR assay uses a pFmiR-3'UTR plasmid sensor to identify regulatory miRNA-target interactions. Traditional cloning method has been used to clone pFmiR-3'UTR plasmid sensor for MGAT3 (**Figure 2-1**). The sensor contains genetically encoded dual-color fluorescent reporter proteins- cerulean and mCherry. 3'UTR sequence of MGAT3 was cloned downstream of cerulean which acts as the positive control. The second fluorescent protein mCherry acts as the negative control. The plasmid sensor is co-transfected with a library of 2601 miRNA mimics into HEK293T cells in 384 well plate format. The miRNA library contains the known human miRNAome as defined by miRBase.<sup>4</sup> The current miRBase version of complete human miRNAome is V.22.1 and here we used the version V.22.0. Thus virtually all known human miRNAs were represented in our assay. All miRNAs are aliquoted in triplicates across 24 plates. All plates also contain six replicates of non-targeting control (NTC) miRNA. After 48 hours of transfection, each well is scanned to obtain ratio of cerulean and mCherry expression. A higher ratio corresponds to the high expression of cerulean due to MGAT3 upregulation and a lower ratio corresponds to the low expression of cerulean compared to mCherry due to down-regulation of MGAT3. The data analysis process is discussed in detail in materials and methods section.

It is important to note that most of the mammalian genes express more than one transcript often generated as a result of alternative splicing. More than 70% of human genes are known to express transcript variants.<sup>43</sup> Multiple transcript variants can have altered biological effect and regulation mechanisms. Recent studies have shown that transcript variants frequently determine changes in 3'UTR length. Multiple variations of mature RNA transcripts that differ in their 3' ends may encode for the same protein, differences in the transcript's 3' end can impact the final protein's level, localization, and its ability to interact with other molecules such as miRNAs, RNA binding proteins etc.<sup>44</sup> It is not clear if MGAT3 has alternative 3'UTR isoforms, but multiple transcriptomic analysis identified alternative variants of MGAT3 expressed in different cancer tissues and cell lines. For MGAT3, three different alternative transcript variants have been identified that encode the same protein. To clone pFmiR-3'UTR plasmid sensor of MGAT3, the most prevalent transcript variant (Ensembl ID: ENST00000341184.7, RefSeq ID: NM\_002409.5) was used for 3'UTR sequence. The most prevalent transcript variant of MGAT3 contains 5394 base pair coding 533 amino acid. In other variants, a truncated version of mRNA transcript and protein coding has been identified.

Downstream validation experiments to test miRFluR assay data in a biological environment include Western blot, reverse transcription quantitative PCR (RT-qPCR) analysis, *Phaseolus vulgaris* Erythroagglutinin (PHA-E) lectin staining and site directed mutagenesis experiment discussed in details in materials and methods section. Here we used three different mammalian cancer cell lines- HT29 (human colorectal adenocarcinoma cell line), A549 (human lung adenocarcinoma) and PANC1 (human

pancreatic ductal adenocarcinoma) to observe miRNA mediated regulation of MGAT3 protein and bisecting GlcNAc.

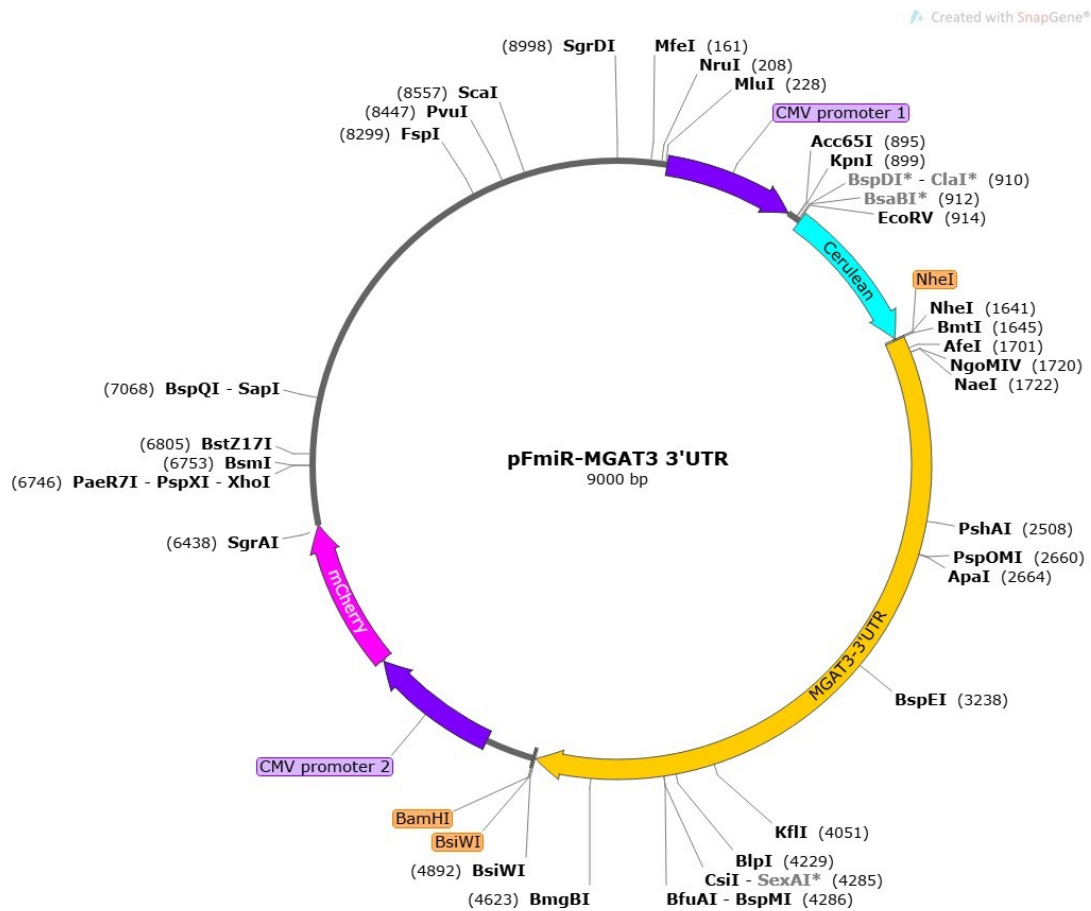


**Figure 2-1: Plasmid map for pFmiR-3'UTR sequence of MGAT3**

The selection of mammalian cancer cell line was based on the expression of MGAT3 in select cells. MGAT3 is a low abundance gene, with moderate to high expression in brain, small intestine and placenta.<sup>45,46</sup> However, recent studies has shown that MGAT3 is highly associated with hepatocellular carcinoma and pancreatic

cancer acting as a tumor suppressor and oncogene respectively.<sup>47,48</sup> A549 cell line has been found to be associated with multiple miRNA hits from miRFluR assay that are discussed in results and discussion chapter. Altogether, all three cell lines hold significant importance relevant to the regulation of MGAT3 and associated miRNA his. Hence, these cell lines were selected for downstream validation experiments.

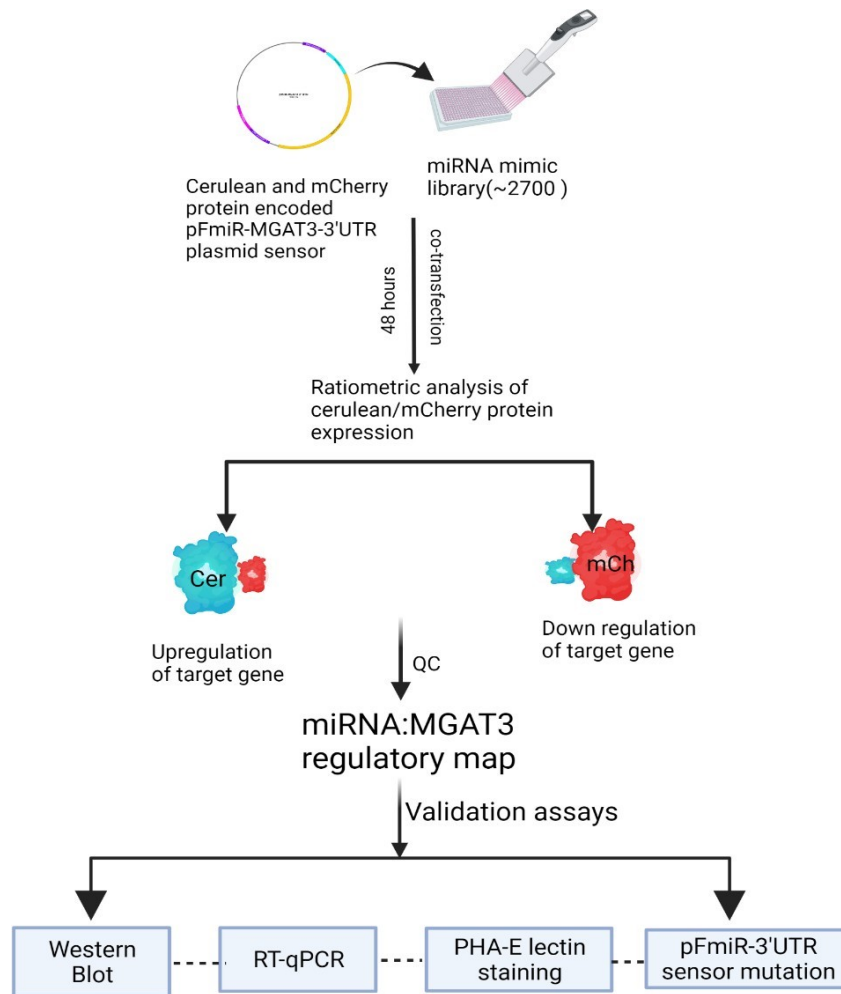


**Figure 2-2. Experimental workflow of miRFluR assay.**

## 2.2. Materials and methods

### 2.2.1. Cloning

Genomic DNA of HEK293t cells was extracted using QIAquick gel extraction kit according to manufacturer's guide. It was then subjected to PCR analysis using forward and reverse primers specific to the 3'UTR sequence of MGAT3 (**Table-1**). The PCR products were cleaned up using PCR clean-up kit from TruIn Science. PCR fragments and empty pFmiR backbone were subjected to restriction enzyme digestion and using 1 unit of High-Fidelity (HF<sup>®</sup>) restriction enzymes NheI and BamHI (from NEB) in 1× rCutSmart<sup>™</sup> NEB buffer at 37°C for 1 hour. Digested fragment and pFmiR backbone were then ligated using 2 µL of T4 DNA ligase in 10× T4 DNA ligase buffer (NEB). The newly synthesized pFmiR-3'UTR construct was then transformed into High-efficiency NEB<sup>®</sup> 10-beta Competent *E. coli* (DH10-β *E. coli* derivative) cells and plated on Carbenicillin LB agar plates for colony formation. Few colonies were verified by colony PCR followed by gel electrophoresis. PCR amplified products of select colonies were sent to Molecular Biology Service Unit, University of Alberta, for Sanger sequencing. Upon verifying the expected pFmiR-3'UTR sequence of the construct, large scale endotoxin free preparation of DNA was performed using QIAGEN miniprep and maxiprep kits. The sequence of MGAT-3'UTR is shown in Appendix-1 section.

**Table-1.** Primer list for cloning pmiR-MGAT3-3'UTR sensor

Primer list	5'- 3'
MGAT3-Fwd	CGTGAGCTAGCCCAAGTACCTGCTGAAGAAC
MGAT3-Rev	CATCAGGATCCCAGACTTTGTAGCTGTTTTTATTATTAATAT

### 2.2.2. Cell culture

Mammalian cancer cell lines- HEK293T, HT29, A549 and PANC1 were purchased from American Type Culture Collection (ATCC). The cells were cultured and maintained in following media- HEK293T, HT29 and PANC1 cell line: Dulbecco's Modified Eagle Medium (DMEM) with 10% Fetal Bovine Serum (FBS), A549 cell line: F-12K (Kaighn's) Medium with 10% FBS. All cells were cultured under standard conditions (5% CO<sub>2</sub> , 37°C). Cell passage number used in all experiments were below 15.

### 2.2.3. miRFluR assay

**Assay method:** The human miRNA mimic library of 2601 miRNAs was purchased from Dharmacon. The miRNAs were resuspended in ultrapure nuclease free water and aliquoted into black 384 well, clear optical bottom tissue culture treated plates (Nunc). Each plate contained three replicate wells of each miRNA in that plate (1.8 pmol/well). In addition, each plate contained a minimum of 6 wells containing non targeting control (NTC). To each well, 30 ng of pFmiR-3'UTR plasmid was added

diluted in 5  $\mu$ l OptiMEM (Gibco). 0.1  $\mu$ l Lipofectamine<sup>TM</sup> 2000 (Life Technologies) was diluted in 5  $\mu$ l OptiMEM (Gibco) and incubated at room temperature for 5 minutes. Then the lipofectamine solution was added to each well. The solution mixture was then allowed to incubate at room temperature for 20 min. HEK293T cells (25  $\mu$ l per well, 10000 cells/well in phenol red free DMEM with FBS 10%) were then added to the plate. Plates were incubated at 37°C, 5% CO<sub>2</sub>. After 48 hours, the fluorescence signals of Cerulean (excitation: 433 nm; emission: 475 nm) and mCherry (excitation: 587 nm; emission: 610 nm) were measured using a plate reader (SYNERGY H1, BioTek, Gen 5 software, version 3.08.01).

**Data analysis:** For data analysis, each well of each plate was scanned by plate reader to measure the fluorescence expression of cerulean and mCherry. Then the expression of cerulean was divided by mCherry expression for each well. Each miRNA contained three replicates of cerulean/mCherry ratio values. The mean ratio, standard deviation (SD) and % error ( $100 \times \text{SD}/\text{mean}$ ) were then calculated for each miRNA. At this stage, miRNAs were subjected to a quality control (QC) process where any miRNA with 15% or higher error was eliminated from the final data analysis. Additionally, if any plate had more than 50% of its total miRNA eliminated, that particular plate was also removed from the final data analysis. A total of 1600 miRNAs passed the QC from the library of 2601 miRNAs. The mean ratio of each miRNA in a plate was then divided by the mean ratio for NTC of that particular plate to calculate the normalized value and the error was propagated within that plate. Data from all plates were then combined and z-score was calculated.

A z-score of  $\pm 1.96$  (95% confidence interval) is usually the standard cut-off for

the down-regulatory (down-miRs) in our previous works<sup>5,16</sup>. However, in this particular case only 2 miRNAs passed the standard threshold. So to test more miRNAs, we decided to set a z-score of  $\pm 1.440$  (85% confidence interval) as initial threshold for both down-miRs and up-miRs. Similar to our previous miRFluR assay investigation, a significant number of miRNAs were found across the dataset that induced MGAT3 upregulation. These upregulatory miRNAs (up-miRs) were subjected to special consideration as very few studies can be found on the mechanism of miRNA-mediated upregulation. The miRNAs selected for post-assay validation experiments were from different regions of the dataset representing both down-regulatory and up-regulatory effects. The selection was based on the data obtained as well as the literature review which is discussed in results and discussion section in details.

#### **2.2.4. Western blot**

miRNA mimics and miRNA hairpin inhibitors (anti-miRs) were purchased from Dharmacon and resuspended in nuclease free water according to manufacturer's guide. MGAT3 antibody was purchased from Proteintech (rabbit, polyclonal, catalogue: 17869-1-AP). Cells were seeded onto 6 well plates with appropriate media at a density of 60000cells/well for HT29, 80000 cells/well for A549 and 100000 cells/well for PANC1 and cultured for 24 hours. 50 nM miRNA mimics and anti-miRs (diluted in 250  $\mu$ L Optimem) were then added to the cells followed by the addition of 5  $\mu$ L of Lipofectamine<sup>TM</sup> 2000 (Life Technologies) diluted in 250  $\mu$ L Optimem and cells were incubated in room temperature for 20 minutes. 1500  $\mu$ L of fresh culture media was then added to the cells. The transfection media was aspirated and fresh media was added

again after 12 hours post transfection to ensure cell viability. After 48 hours, the cells were washed with PBS and lysed with ice-cold NP-40 (nonionic polyoxyethylene surfactant) lysis buffer with protease inhibitors (Pierce™ Protease inhibitor tablets from Thermo Scientific™). The protein concentration of whole lysate was measured by BCA assay (Micro BCA assay kit, Invitrogen). For Western blot, 50µg protein in was run in each well of 10% SDS-PAGE gel. Proteins were denatured in 4× Laemmli sample buffer containing β-mercaptoethanol at 95°C for 5 minutes before running in the gel. The proteins were then transferred to iBlot2 Transfer Stacks (nitrocellulose, Invitrogen) using the iBlot2 transfer device (Invitrogen). Blots were incubated with Ponceau S Solution for 10 minutes and the total protein levels were imaged using gel imager (Azure 600, Azure Biosystems Inc.).The blots were then blocked with 10% non-fat dry milk in TBST (TBS buffer with 0.1% Tween 20) buffer at room temperature on a platform rocker at 60 rpm. After 2 hours of blocking, the blots were treated with primary anti-MGAT3 antibody (from Proteintech; rabbit, polyclonal, catalogue: 17869-1-AP) at 1:1000 dilution in TBST at 4°C overnight. Blots were then washed with TBST 4×, 2 minutes. After washing, a secondary antibody (anti-rabbit IgG-HRP) was added at a dilution of 1:10000 in TBST. Blots were then incubated on platform rocker at 60rpm for 1 hour at room temperature. After the incubation, the blots were again washed with TBST buffer for 4×, 2 minutes. The blots were then developed using Clarity and Clarity max Western ECL-substrate (from Bio-Rad) according to manufacturer's instruction. The blots were imaged using a gel imager (Azure 600, Azure Biosystems Inc.) choosing the chemiluminescent option. All Western blots were quantified with ImageJ software. All experiments were done in biological triplicate.

### 2.2.5. RT-qPCR

Cells were treated with miRNA mimics as described in the Western blot section. After 48 hours of transfection, cells were lysed with TRIzol reagent (Invitrogen) for total RNA extraction according to manufacturer's guide. RNA concentrations were measured using NanoDrop. Isolated RNA was then reverse-transcribed to synthesis cDNA using Superscript III Cells Direct cDNA synthesis kit (Invitrogen) following manufacturer's instruction. Syber Green method was used for RT-qPCR analysis and cycle threshold (Ct) values were obtained using Applied Biosystem (ABI) 7500 Real-Time PCR machine and normalized to GAPDH, a housekeeping gene. The primers used for MGAT3 and GAPDH are listed in table-2. All experiments were done in three biological replicates.

**Table-2. Primer list for RT-qPCR**

Primer list	5'- 3'
MGAT3-qPCR-Fwd	AGTGGGTTGAGTGTGTGTGC
MGAT3-qPCR-Rev	CTCGTGGTTGATGTTGATGG
GAPDH-qPCR-Fwd	ACCACAGTCCATGCCATCAC
GAPDH-qPCR-Rev	TCCACCACCCTGTTGCTGTA

### 2.2.6. PHA-E lectin staining

*Phaseolus vulgaris* Erythroagglutinin (PHA-E) is a legume lectin that has high specificity toward biantennary glycosylated N-glycan with bisecting GlcNAc. It is often used in glycobiology applications to see the presence of bisecting GlcNAc in a

given sample. Fluorescein (Fl) conjugated PHA-E lectin was purchased from Vector Laboratories. For cell culture, sterile 22×22 no. 1 coverslips were placed onto 6 well plates or, 35 mm dishes. Cells were then seeded and treated with miRNA mimics as described in the Western Blot section. At 48 hours post-transfection, cells were washed with 1 ml sterile PBS buffer 3×. Cells were then fixed with 4% para-formaldehyde in sterile PBS buffer at room temperature for 15 minutes. After the fixation, cells were again washed with sterile PBS buffer for 3×. FITC conjugated PHAE lectin (Vector Laboratories) was then added to the cells at a dilution of 1:500 in PBS. Cells were incubated at 4°C in dark. After 1 hour of incubation, cells were again washed with PBS (3×) and each well was counterstained with 1 µL of Hoeschst 33342 (Invitrogen) at room temperature for 10 minutes in dark. The coverslips were then mounted onto slides with mounting media (90% glycerol in PBS) and imaged with a Zeiss fluorescent microscope (Camera: Axiocam 305 mono, software: ZEN 3.2 pro). PHA-E lectin staining assay was performed in HT29 and A549 cell lines at a minimum of 2 biological replicates. To confirm the appropriate staining and rule out the possibility of non-specific fluorescence, some cells were treated with PNGase F enzyme (cleaves almost all N-linked glycans from glycoproteins) prior to staining according to manufacturer's instruction (NEB).

### **2.2.7. Site directed mutagenesis**

3'UTR sequence of MGAT3 and hsa-miR-92a-1-5p (up-miR) sequence were analyzed with RNAhybrid<sup>49</sup> to get the predicted binding interaction site. RNAhybrid calculates the maximum free binding energy between a miRNA and target mRNA

sequence. The most stable predicted site for miR-92a-1-5p had a free energy of -33.3 kcal/mol. I mutated this site to determine whether the miR-92a-1-5p has a direct binding effect on MGAT3. Primers for mutated sequence were designed using NEBaseChanger<sup>TM</sup> tool (**Table-3**). Site-specific mutagenesis reaction was carried out using Q5<sup>®</sup> Site-Directed Mutagenesis Kit from New England Biolabs inc. following the manufacturer's guide. The mutant plasmid was then transformed into *E. coli* bacterial cells for amplification. The mutated sequence was verified by gel electrophoresis followed by Sanger sequencing (Molecular Biology Service Unit, University of Alberta). miRFluR assay was then performed for the mutant sensor along with the wild type sensors. A minimum of 3-wells for miR-92a-1-5p and 3-wells for NTC were transfected for each sensor. Mean ratio of cerulean/mCherry expression was calculated for miR-92a-1-5p and NTC of both sensors. The ratio of miR-92a-1-5p of each sensor was first normalized to respective NTC and then the mutant sensor data was compared to wild type sensor. The sequence of mutated sensor is attached in Appendix 2.

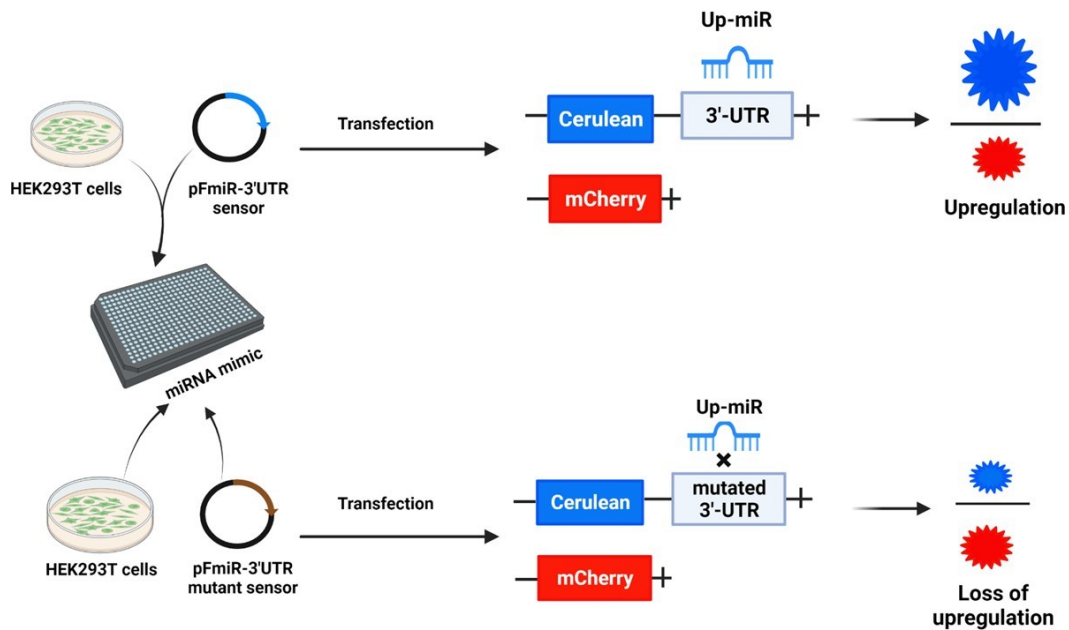


**Figure 2-3: Schematic representation of site specific mutation experiment of pFmiR-3' UTR sensor.** Mutation of miRNA binding site in 3'UTR of target mRNA causes a loss of regulation for up-miRS. If the miRNA does not have a direct binding effect on target gene then no change in regulation is seen.

**Table-3.** List of primers for cloning mutated pFmiR-3'UTR sensor

Primer list	5'- 3'
Mut-92a-1-5p-Fwd	CTACCTCCCCAGCCCCTC
Mut-92a-1-5p-Rev	TCAGGTCAGGATTCTCATTCTCAG

## Chapter 3: Results and Discussion

### 3.1. MGAT3 is predominantly upregulated by miRNAs in miRFluR assay

To understand the role of miRNA in MGAT3 regulation, we conducted a high-throughput miRFluR assay to map the complete regulatory network of miRNAs for MGAT3. Data analysis reveals that miRNA mediated upregulation is the most dominant regulatory action of miRNAs on MGAT3. A library of 2601 miRNAs was screened for the assay from which a total of 1542 miRNAs passed the quality control process. In the final analysis, we identified 125 miRNAs hitting the cut-off for both downregulation and upregulation (**Appendix-5**) which is 8% of the total miRNAs that passed QC. We identified 15 down-miRs and 110 up-miRs in final dataset using our cut-off. The number of down-miRs in the assay is surprisingly low in contrast to the popular notion of miRNA mediated repression. Interestingly, we found a significant number of miRNAs upregulating MGAT3 which is 88% of total miRNA hits. When compared to TargetScan, one of the most used miRNA prediction algorithms, only two down-miRs from the assay were predicted by TargetScan as miRNA hit for MGAT3. On the other hand, 28 up-miRs from the assay were predicted by TargetScan but as down regulatory miRNAs (context++ score >50). There are two miRNA hits found from literature review- has-miR-23a-3p and has-miR-188-5p.<sup>47,50</sup> However, both of these miRNAs did not pass the QC in miRFluR assay.

There are not many studies related to the miRNA-mediated gene activation process. Very few studies reported miRNAs activating gene expression but most of them were in quiescent cells or any other particular cellular state.<sup>13,14</sup> However, from

our assay, it is evident that miRNAs may activate gene expression in normal proliferating cells. MGAT3 is responsible for catalyzing the addition of a bisecting GlcNAc to the beta 1-4 linkage of core tri-mannose residue of N-glycan. Addition of a bisecting GlcNAc is extremely significantly as it changes both the composition and conformation of N-linked glycans. The presence of bisecting GlcNAc interferes with other N-linked branching enzymes especially, MGAT5<sup>39,51</sup> which is highly associated with tumor malignancies.<sup>52</sup> miRNAs predominantly upregulating MGAT3 may help us to modulate the regulation of N-linked glycan branching in general to control tumor malignancies.

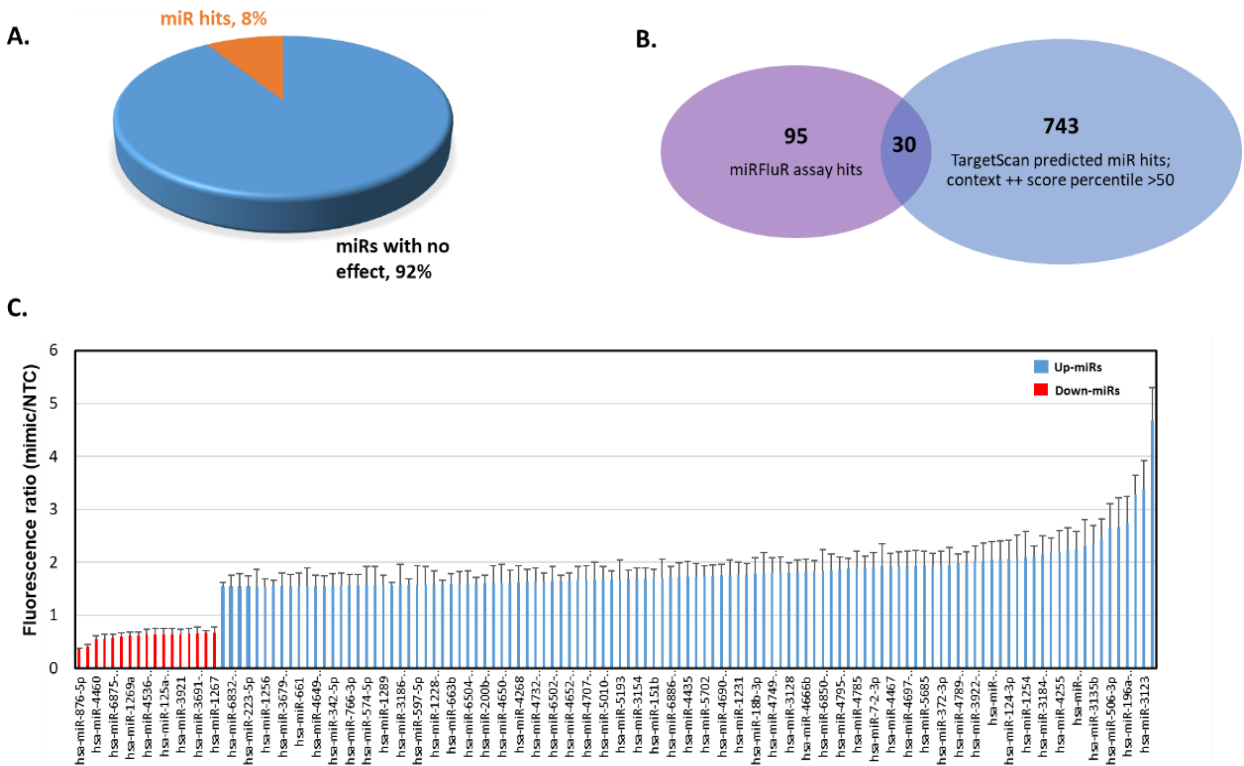


**Figure 3-1: miRFluR assay data analysis.** A) The percentage of miRNA hits compared to the total miRNAs that passed quality control process. B) Comparison of

miRFluR assay data with predicted hits from TargetScan for MGAT3. Only 30 miR hits from assay matches with predicted hits from TargetScan that may interact with MGAT3. Predicted hits from TargetScan represent context++ score percentile of >50. C) Bar graph of miRNA hits for MGAT3. The data are normalized to NTC. Error bars represent propagated error.

### **3.2. Selection of miRNAs for post-assay validation experiments**

To validate miRFluR assay data, we initially selected 16 miRNAs from the miRFluR dataset (**Table-4**). Five of them are down-miRs and eleven of them are up-miRs. miRNAs were chosen on the basis of data obtained from miRFluR assay and literature review. Literature review of miRNA hits for MGAT3 revealed them to be highly enriched in cancer pathways. For example, miR-876-5p has a tumor suppressive role in breast cancer and hepatocellular carcinoma.<sup>53,54</sup> It was also the highest hit for MGAT3 downregulation in miRFluR assay. In a recent study, miR-let-7g-5p has been identified as a tumor suppressor and predictive biomarker for chemo-resistance in human epithelial ovarian cancer.<sup>55</sup> Interestingly, MGAT3 and corresponding bisecting GlcNAc level has also been associated with poor survival of ovarian cancer patients.<sup>38</sup>

Among all the selected up-miRs, most significant ones are miR-661, miR-889-5p, miR-146b-3p, miR-212-5p, miR-124-3p, miR-92a-1-5p. All of them have been associated with multiple cancer progression and metastasis. High level of miR-661 has been identified in non-small cell lung carcinoma.<sup>56,57</sup> miR-889-5p is highly expressed in hepatocellular carcinoma and has been linked with poor prognosis and cancer metastasis. MGAT3 is a known suppressor for hepatocellular carcinoma. This indicates

a potential role of this up-miR in regulating MGAT3 and corresponding bisecting GlcNAc in liver cancer metastasis. miR-92a-1-5p is another significant up-miR which is the highest hit for MGAT3 upregulation in miRFluR assay data. High expression of miR-92a-1-5p has been linked with poor prognosis, increased cell proliferation and metastasis of cervical cancer and osteosarcoma.<sup>58,59</sup> It has also been reported to suppress non-small cell lung carcinoma in a synergistic effect with miR-18a.<sup>60,61</sup> miR-212-5p is associated with poor prognosis of breast cancer and have been identified to upregulate  $\alpha$ -2,6-sialic acid through direct miRNA-mRNA interaction.<sup>16</sup>

Not all miRNAs selected for post-assay validation experiments were within the cut-off. miR-544b (down-miR), miR-146a-3p (down-miR) and miR-221-5p (up-miR) were chosen outside the cut-off. miR-544b and miR-146a-3p were just below the cut-off. As MGAT3 had a low number of down-miR hits, I wanted to test if the miRNAs that did not meet the cut-off had any effect on MGAT3. miR-221-5p was chosen because it was validated as an up-miR for ST6GAL1 in previous work from our lab.<sup>16</sup> miR-221-5p is highly expressed in pancreatic cancer and prostate cancer leading to decreased survival.<sup>62,63</sup>

**Table-4: Selected miRNA hit list of MGAT3 for post-assay validation experiments**

miRNA	Normalization over NTC	Z-score
hsa-miR-876-5p	0.380980345	-2.35311
hsa-let-7g-5p	0.609172463	-1.60088
hsa-miR-3921	0.643201496	-1.48871
hsa-miR-544b	0.66227508	-1.42583

hsa-miR-146a-3p	0.671871185	-1.3942
hsa-miR-221-5p	1.365773253	0.893218
hsa-miR-661	1.54861416	1.495945
hsa-miR-1289	1.566160006	1.553784
hsa-miR-146b-3p	1.839291916	2.454152
hsa-miR-212-5p	1.917495578	2.711947
hsa-miR-129-1-3p	1.930104976	2.753514
hsa-miR-124-3p	2.071235	3.218743
hsa-miR-1254	2.087367629	3.271923
hsa-miR-3135b	2.329111195	4.068821
hsa-miR-889-5p	2.43548965	4.419493
hsa-miR-92a-1-5p	4.674151271	11.79915

### 3.3. Western Blot validation in mammalian cancer cell lines

To validate the miRFluR assay data, we performed Western blot experiments on three different mammalian cancer cell lines- HT29, A549 and PANC1. miRNA mimics of selected assay hits (discussed in previous section) were overexpressed in these particular cell lines through transient transfection and MGAT3 protein regulation was checked through Western blot. The results showed majority of miRNA mimics reproducing assay data in cancer cells. 16 miRNAs were tested in HT29 cell line where hsa-miR544b, has-miR-146a-3p and hsa-miR-221-5p were also tested to check whether miRNAs that did not make the cut-off have effect on protein regulation. The results in HT29 cell line were completely in line with the assay data. In line with the

previous works from our lab, MGAT3 was significantly upregulated by some up-miRs in HT29 particularly by miR-92a-1-5p, miR-124-3p, and miR-889-5p when compared to non-targeting control (**Figure 3-2**).

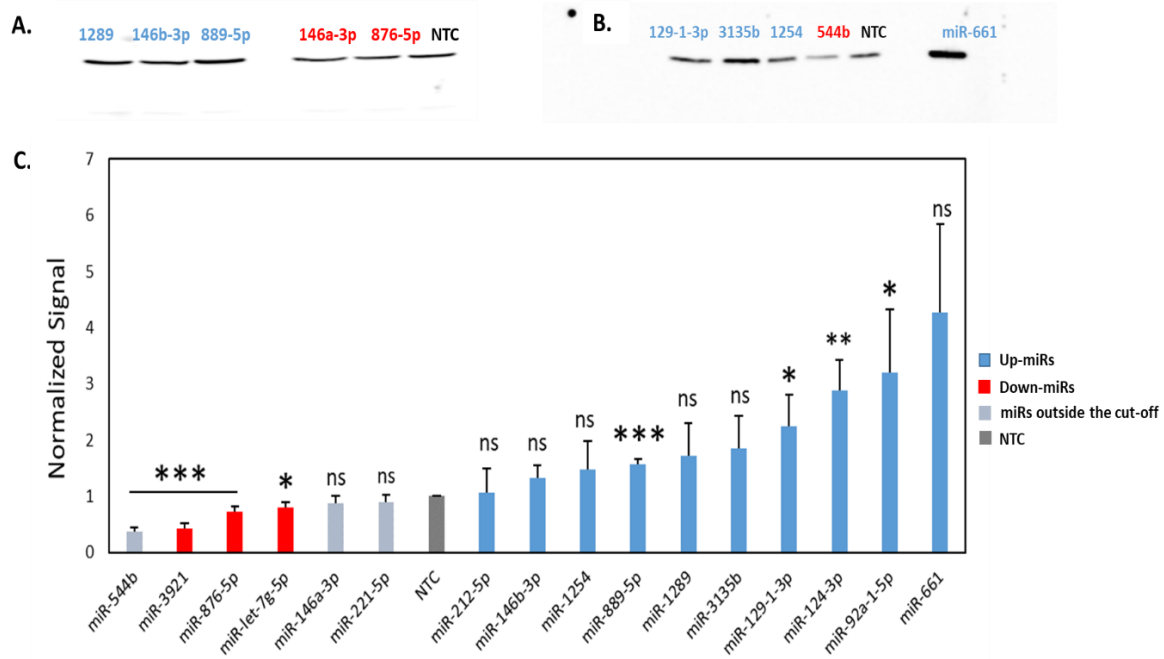


**Figure 3-2: Western Blot validation data in HT29.** miRNA mimics of miRFluR assay hits were tested in HT29. A) and B) shows representative blots for MGAT3 (at 61 kD). D) Western blot quantification data in HT29. MGAT3 expression was normalized to Ponceau and divided by the normalized signal of NTC. All experiments were performed in biological triplicate. Errors shown are standard deviations. Paired t test was used to compare miRNAs to NTC (ns: not significant, \*  $p < 0.05$ , \*\*  $< 0.01$ , \*\*\*  $< 0.001$ ).

MGAT3 protein regulation was seen to vary in PANC1 cell line. Compared to downregulation, upregulation of MGAT3 was more consistent with the assay result in

however, statistical analysis did not find much significant data (**Figure 3-3**). miRNA mimics are chemically synthesized exogenous molecule which in few cases may also cause perturbation of bigger regulatory network causing disruption in gene regulation. This is also crucial for the regulation of low abundance genes like glycogenes. For example, several transcriptomic profiling of PANC1 and other pancreatic cancer cell lines revealed very low expression of MGAT3. In contrast to transcriptomic data, MGAT3 has been reported as one of the most significant and highly expressed glycosylation enzymes (on protein level) in pancreatic cancer modulating the cancer progression.<sup>45,64,48</sup> The difference in transcriptomic and proteomics data in pancreatic cancer is perhaps reflecting the presence of more complex regulatory network of MGAT3 in pancreatic cancer that may result in a discrepancy of miRNA mediated regulation on cellular level.

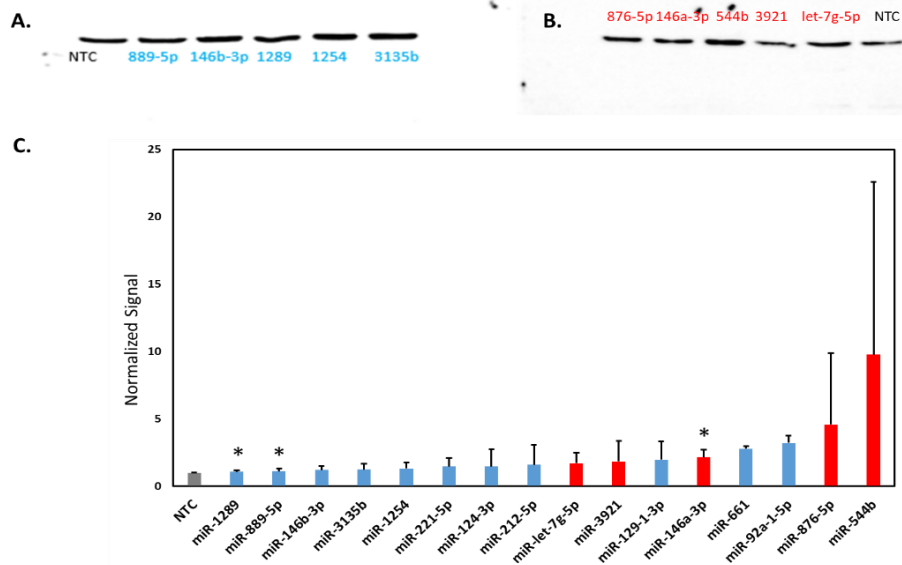


**Figure 3-3: Western Blot validation data in PANC1.** miRNA mimics of miRFluR assay hits were tested in PANC1. A) and B) shows representative blots for MGAT3 (at

61 kD). D) Western blot quantification data in PANC1. MGAT3 expression was normalized to Ponceau and divided by the normalized signal of NTC. All experiments were performed in biological triplicate. Errors shown are standard deviations. Paired t test was used to compare miRs to NTC (ns: not significant, \*  $p < 0.05$ , \*\*  $< 0.01$ , \*\*\*  $< 0.001$ ).

In A549 cell line, I only tested six miRNA hits which also showed a consistent result with miRluR assay data except for miR-661 which showed a significant upregulation of MGAT3 in HT29 (**Figure 3-4**).

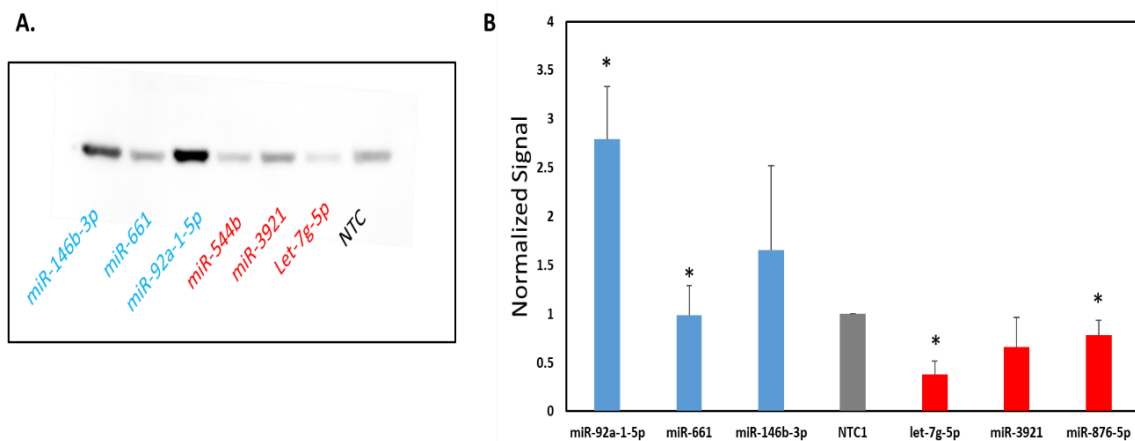


**Figure 3-4: Western Blot validation data in A549.** miRNA mimics of miRFluR assay hits were tested in A549. A) and B) shows representative blots for MGAT3 (at 61 kD). D) represents Western blot quantification data in A549. MGAT3 expression was normalized to Ponceau and divided by the normalized signal of NTC. All experiments were performed in biological triplicate. Errors shown are standard deviations. Paired t test was used to compare miRs to NTC (ns: not significant, \*  $p < 0.05$ , \*\*  $< 0.01$ , \*\*\*  $< 0.001$ )

Western blot data for MGAT3 in three different cell lines indicate miRNAs may act as cell dependent manner for the regulation of target gene. To test the effect of endogenous miRNAs on MGAT3 regulation, we next performed Western blot experiment of anti-miRs in HT29. Anti-miRs or, antagomiRs are chemically synthesized oligonucleotides designed to inhibit the effect of corresponding endogenous miRNA in a biological environment. They are also known as hairpin inhibitors of miRNAs. Anti-miRs of selected miRNAs were transfected into HT29 cells and the MGAT3 protein level was evaluated (**Figure 3-5**).

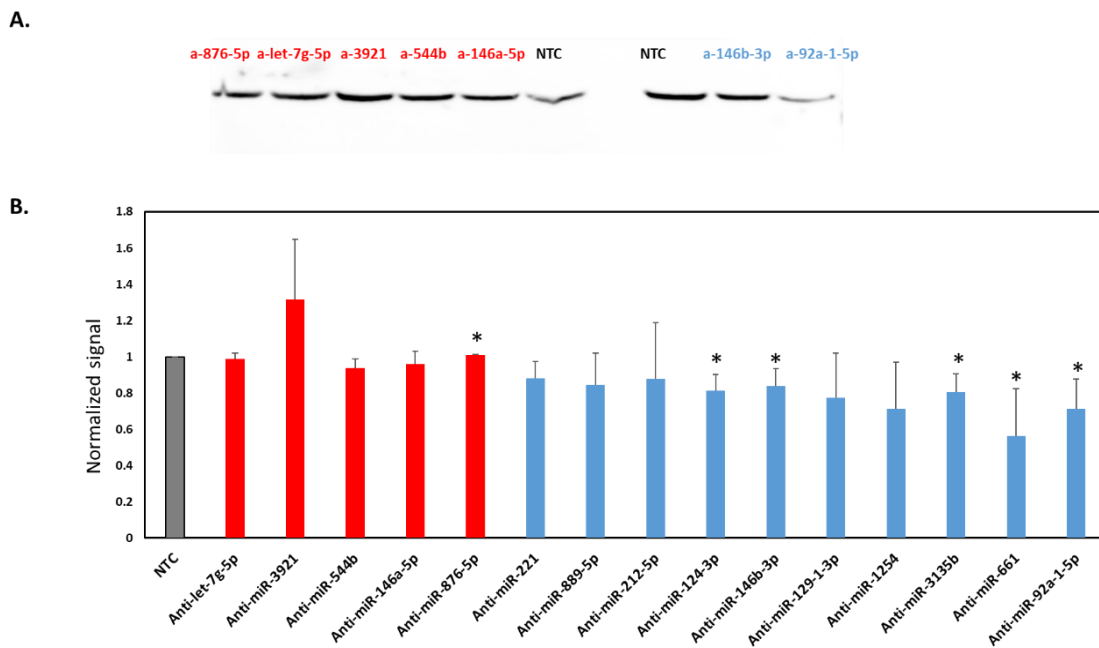


**Figure 3-5: Western blot validation data for anti-miRs.** Anti-miRs were tested in HT29 to evaluate the effect of endogenous miRNAs on MGAT3 A) representative blots for anti-miRs. B) quantitative Western blot data for selected anti-miRs in HT29. MGAT3 expression was normalized to Ponceau and divided by the normalized signal of NTC. All experiments were performed in biological triplicate. Errors shown are

standard deviations. Paired t test was used to compare miRs to NTC (ns: not significant, \*  $p < 0.05$ , \*\*  $< 0.01$ , \*\*\*  $< 0.001$ ). Anti-down miRs and anti-up miRs are color coded as red and blue respectively.

The result indicates small amount of change in MGAT3 protein level in HT29 for all down-miRs and some of the up-miRs. miR-661 upregulated MGAT3 in HT29 significantly in Western blot. Transfecting HT29 with anti-miR-661 reverted the protein regulation in statistically significant level. Loss of upregulation was also seen for miR-92a-1-5p, miR-146b-3p, miR-124-3p.

#### **3.4. RT-qPCR data in HT29 and A549 cell line**

RT-qPCR analysis was performed in HT29 and A549 cell lines for selected miRNAs to evaluate the effect of miRNAs on MGAT3 mRNA level. However, transcript levels do not always accurately reflect protein abundance, particularly for low abundance genes such as glycogenes and cell surface receptors. These genes are known to have low transcript levels but high protein abundance. Therefore, changes in transcript levels may not necessarily correspond to changes in protein levels in response to microRNAs. In fact, the correlation between changes in transcript and protein levels in response to microRNAs is much lower for these particular genes.<sup>65</sup> Intriguing results have been observed in cells following perturbation, single cell study relating the difference in protein abundance and transcriptomic level.<sup>66</sup> Although the impact of miRNAs on transcriptomic level is less significant compared to protein level, few studies have reported that more highly repressed targets may exhibit higher level of

mRNA destabilization.<sup>67</sup>

Our data revealed effects of miRNA MGAT3 mRNA level in both HT29 and A549 do not always correspond to the protein level upon as observed in Western blot data. In Ht29, three up-miRs- miR-92a-1-5p, miR-146b-3p, and miR-1254 that significantly increased the protein expression in Western did not have any effect on the mRNA level which was also the case for down-miR let-7g-5p. In A549, data RT-qPCR data was more in line with data from Western blot or miRFluR assay. In summary, both cases were observed where miRNAs are regulating both mRNA and protein level in the same direction or impacting the protein level having no effect on mRNA level. Although a higher error was noticed in both datasets.

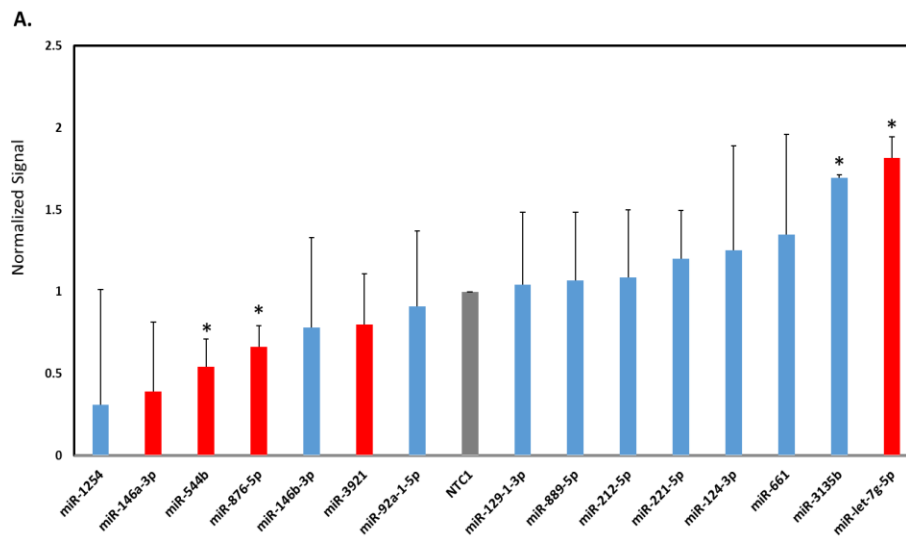


**Figure 3-6: RT-qPCR data in HT29 cell line.** A) represents RT-qPCR data in HT29. Down-miRs and up-miRs are color coded in red and blue respectively. Data represents summery of triplicate experiments. All samples were normalized to GAPDH as house-

keeping gene then to NTC. Paired t-test was used to compare miRs to NTC (ns: not significant, \*  $p < 0.05$ , \*\*  $< 0.01$ , \*\*\*  $< 0.001$ ).

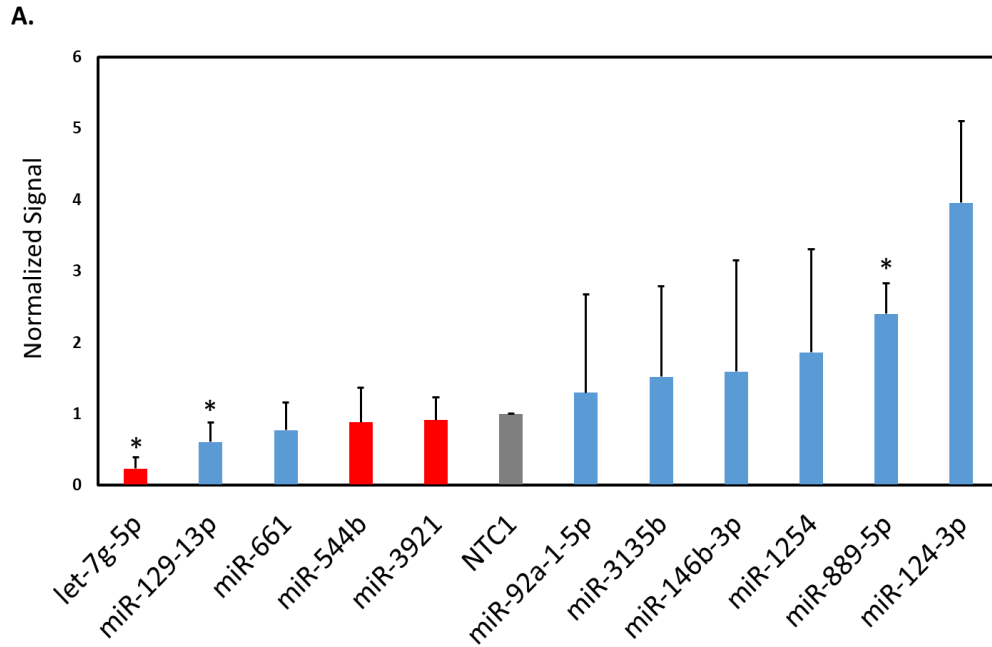


**Figure 3-7: RT-qPCR data in A549 cell line.** A) represents RT-qPCR data in A549 cells. Down-miRs and up-miRs are color coded in red and blue respectively. Data represents summary of triplicate experiments. All samples were normalized to GAPDH as house-keeping gene then to NTC. Paired t-test was used to compare miRs to NTC (ns: not significant, \*  $p < 0.05$ , \*\*  $< 0.01$ , \*\*\*  $< 0.001$ ).

### **3.5. PHA-E lectin staining detects bisecting GlcNAc level follows miRFluR assay**

Phytohemagglutinin from *Phaseolus vulgaris* (PHA-E) is highly specific for biantennary N-glycans bearing bisecting GlcNAc which makes it a very useful reagent in the field of glycobiology.<sup>68</sup> We stained HT29 and A549 cell lines with fluorescein conjugated PHA-E lectin to observe the miRNA regulatory impact on MGAT3. We tested one down-miR and three up-miRs in HT29. hsa-miR-876-5p and hsa-miR-92a-1-5p were the highest hits in miRFluR assay for MGAT3 down-regulation and up-regulation respectively. These miRNAs were also validated by Western blot analysis. So we wanted to check whether the data reflects on the level of bisecting GlcNAc. Additionally, we tested hsa-miR-661 and has-miR-124-3p. miR-661 showed the highest upregulation of MGAT3 in Western blot analysis and miR-124-3p is one of the most highly regulating miRNA, associated with multiple cancer pathogenesis primarily acting as a tumor suppressing miRNA. I observed an increased level of bisecting GlcNAc when cells were transfected with up-miRs and decreased bisecting GlcNAc level for down-miR reflecting miRNA mediated regulation of MGAT3 protein (**Figure 3-8**).

Bisecting GlcNAc regulation in A549 cell line also reflects the miR-mediated regulation of MGAT3 (**Figure 3-9**). miR-146b-3p which moderately upregulated MGAT3 in Western blot analysis, highly increased the level of bisecting GlcNAc level on cell surface level in A549. miR-146b-3p is considered as a prognostic biomarker in lung cancer.<sup>69</sup> Overexpressing miR-146b-3p in A549 may have caused higher regulation of MGAT3 resulting in higher synthesis of bisecting GlcNAc.

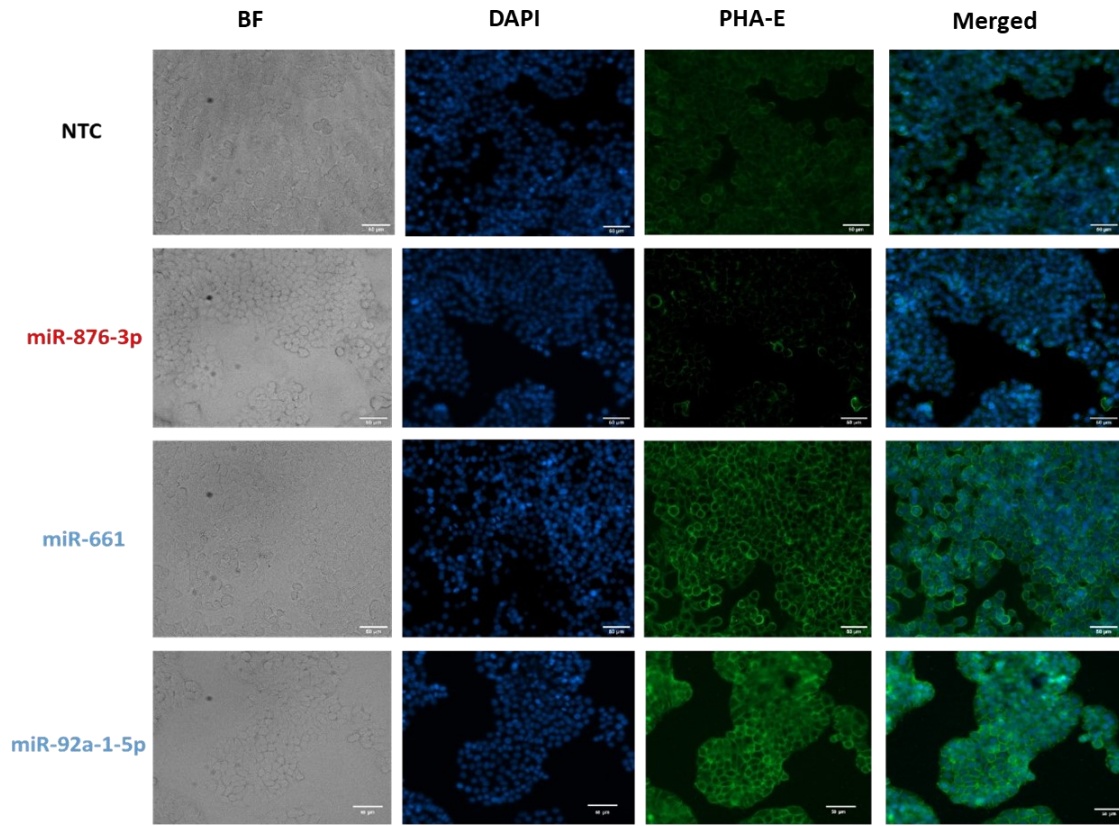


**Figure 3-8: PHA-E lectin staining of HT29 cells.** Change in bisecting-GlcNAc level is consistent with miRFluR assay data. All experiments were performed in biological triplicate. Up-miRs and down-miRs are color coded as blue and red respectively.

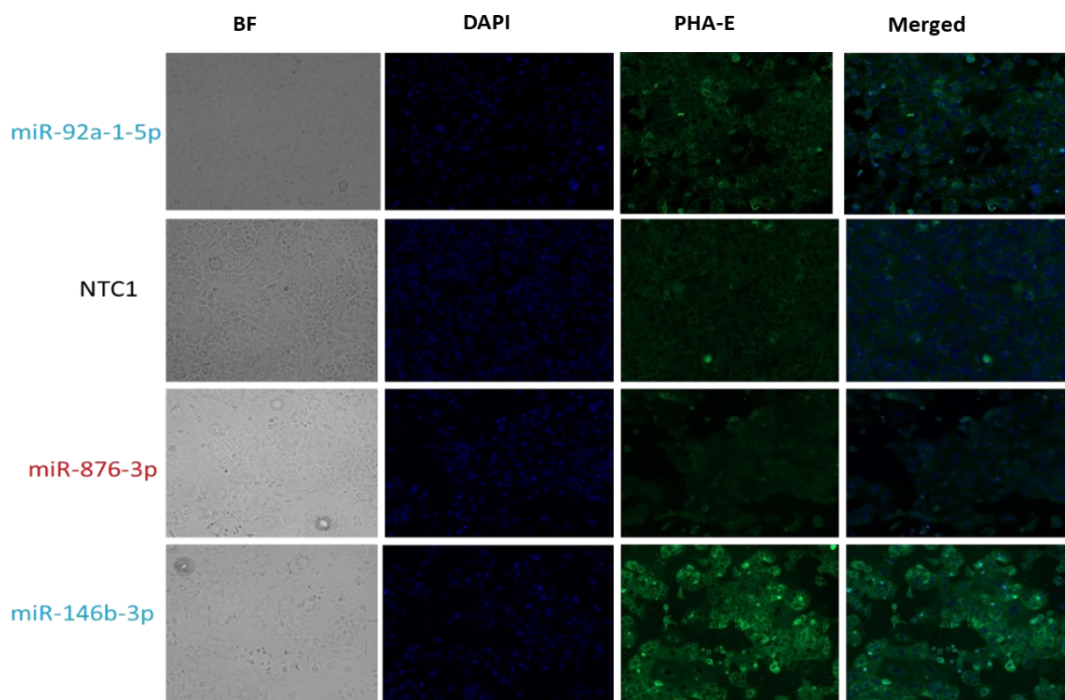


**Figure 3-9: PHA-E lectin staining of A549 cells.** Change in bisecting-GlcNAc level is consistent with miRFluR assay data. Up-miRs and down-miRs are color coded as blue and red respectively. All experiments were performed in two biological replicates.

### **3.6. Site specific mutation of 3'UTR sequence revealed miR-92a-1 5p directly binds to MGAT3 – 3'UTR and mediate upregulation**

The general impression of miRNA regulatory mechanism is that they finely tune protein expression by repressing the target gene. In contrast, we have observed a significant amount of miRNA-mediated upregulation in our assay. Although I have validated the target gene expression at the protein level, it is important to determine the binding interaction between miRNA and target mRNA to show direct interactions.

To test if the miRNA has a direct binding effect, I performed site specific

mutation experiment on the pFmiR-3'UTR sequence of MGAT3 and tested the sensor against miRNA mimic. I focused on miR-92a-1-5p which is highly associated with miR-mediated cancer pathways. miR-92a family has been identified as a potential diagnostic biomarker for lung cancer.<sup>70</sup> miR-92a-1-5p is generally poorly expressed in non-small cell lung cancer. Overexpression of this miRNA has resulted in promoting invasion, metastasis and cellular proliferation of lung cancer, cervical cancer and osteosarcoma.<sup>59-61,70</sup> miR-92a-1-5p upregulated MGAT3 in all three cell lines used in validation experiments. It is also the highest hit for MGAT3 upregulation in miRFluR assay.

To validate miR-92a-1-5p target site in 3'UTR of MGAT3, I analyzed their sequences using RNAhybrid to identify the most stable prediction site. RNAhybrid calculates the minimum free binding energy, also known as hybridization energy, between the miRNA and target mRNA 3'UTR sequence and predicts the most stable interacting sequence. Site predicted for miR-92a-1-5p and MGAT3 located at a site position 2010 in the 3'UTR with a free minimum energy of -33.3 kcal/mol making it highly stabilized. Unlike the canonical miRNA seed region (2-8 nucleotides at the 5' end of miRNA), the site predicted by RNAhybrid did not show seed region complementarity. The predicted site was also high in GC content unlike some studies that reported the presence of AU rich region as a requirement for miRNA mediated upregulation in quiescent cells.<sup>13</sup> To validate the prediction site, I mutated all the interacting base pairs of the 3'UTR region to the corresponding miRNA sequence in the pFmiR-3'UTR plasmid. The mutated sequence was verified by Sanger sequencing. I then tested the mutated sensor along with the original sensor against miR-92a-1-5p

mimic in HEK293T cells. The result showed a significant loss of protein regulation by miR-92a-1-5p upon mutation of the predicted binding site, confirming that miR-92a-1-5p upregulates MGAT3 by directly binding to its 3'UTR.

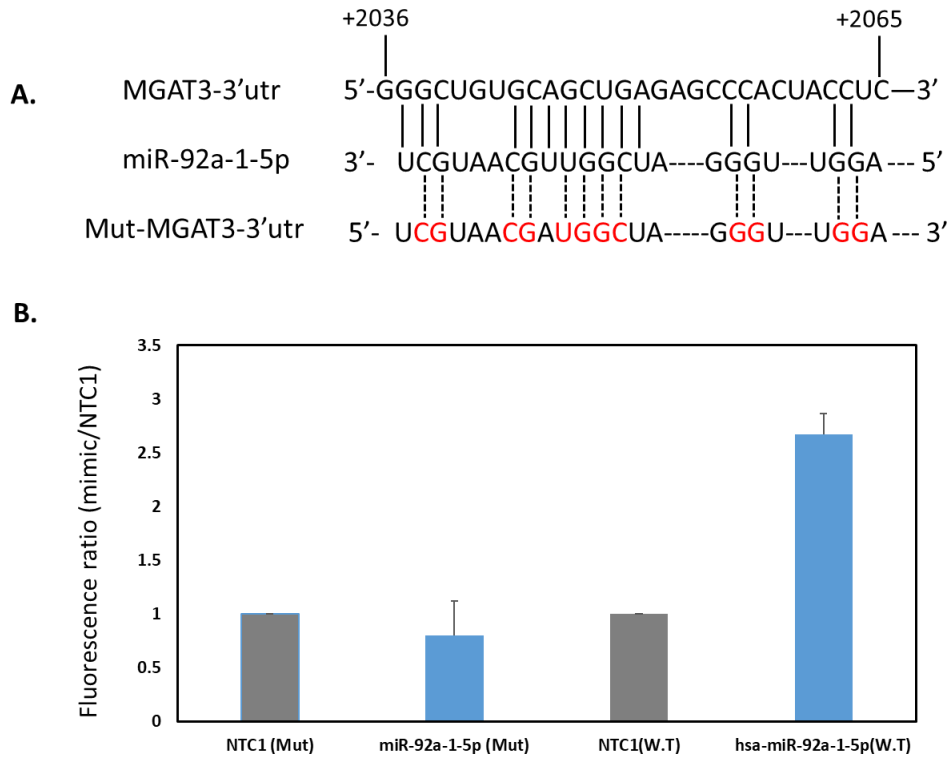


**Figure 3-10: Site specific mutation analysis for miR-92a-1-5p.** A) Represents the binding site for miR-92a-1-5p in MGAT3-3' UTR sequence. The mutated sequence is presented as Mut-MGAT3-3'UTR and mutated nucleotides are color coded as red. B) is the miRFluR analysis data for the mutated plasmid sensor compared with the wild type pmiR-MGAT3-3'UTR plasmid sensor. miRNA mediated regulation is normalized over NTC. Data representative of three biological replicates.

## Chapter 4: Conclusion

Here we aimed to generate a complete miRNA regulatory map for miRNA-MGAT3 interaction by using newly developed miRFluR assay. miRNA targets have been often seen to mimic the biological function of the corresponding miRNA hits. Leveraging this hypothesis we would be able to predict the biological function of MGAT3 once a complete miRNA-MGAT3 interactome is established. First we created a genetically encoded dual color fluorescent plasmid sensor for the 3'UTR sequence of MGAT3. By transfecting the sensor in HEK298t cells with a miRNA library of ~2700 miRNAs, we were able to create a high-throughput “Omics” approach in miRNA regulation study. miRFluR assay revealed MGAT3 to be predominantly upregulated by miRNAs. There are very few studies related to miRNA mediated upregulation of gene expression as opposed to the general impression of miRNA mediated gene repression. A smaller number of luciferase assays were conducted for POT1, PTEN, MXI1 and other cancer related genes where miRNA mediated upregulation was observed. However, they were cancelled out as noise.<sup>71</sup> In previous works from our lab, miRNA mediated upregulation was observed and validated for B3GLCT, ST6GAL1 and ST6GAL2. miRFluR assay findings for MGAT3 also revealed significant amount of miRNA-mediated upregulation of MGAT3. The miRFluR assay finding for up-miRs is significantly important. For downstream validation experiments, these up-miRs were given special consideration.

Next we validated miRFluR assay in three different mammalian cancer cell line - HT29, A549 and PANC1. Western blot data for selected miRNA mimics was consistent with assay data except for PANC1. To our surprise, all up-miRs were found

to upregulate the MGAT3 protein level in HT29 and A549 cell lines indicating this may be a general regulatory mechanism of miRNAs. Next we performed RT-qPCR to evaluate the impact of miRNA hits on MGAT3 mRNA level. Transcriptomic level and protein level of a gene do not always go in accordance. As expected, we saw variation in mRNA levels for both up-miRs and down-miRs. We also tested the effect of endogenous miRNAs on MGAT3 protein level in HT29 by using the hairpin inhibitors of selected miRNAs. miRNA hairpin inhibitors or anti-miRs are designed to competitively block the action of endogenous miRNA. Theoretically, if the endogenous miRs actually bind with target MGAT3, then we will observe a negative regulation for anti-up-miRs and positive regulation of anti-down miRs. The data showed a varied regulation for both anti- up and down miRs. The highest repression was observed for anti-miR-661 in HT29 cells. Interestingly, miR-661 was seen to highly upregulate MGAT3 in HT29. PHA-E lectin staining of HT29 and A549 cells also revealed that the level of bisecting-GlcNAC imitate the miR-mediated regulation of MGAT3 for both up and down miRs. The data indicates that miRNA mediated upregulation also impact on the synthesis of bisecting-GlcNAc and may modulate the disease pathways.

To verify if miRNA mediated upregulation occurred by directly binding to the 3'UTR sequence, we created a mutated sensor for miR-92a-1-5p. This is the highest hit for MGAT3 among the up-miRs in miRFluR assay. The mutated sensor was tested against miR-92a-1-5p mimic in the assay comparing with the wild type sensor. The data revealed a significant loss of protein regulation in case of mutated sensor indicating miR-92a-1-5p indeed possesses a direct binding effect on MGAT3 to mediate upregulation.

Most of the miR hits from the assay data are highly enriched in cancer pathways. Up-miRs such as, miR-92a-1-5p, miR-661, miR-146b-3p were identified in association of cancer progression and metastasis of lung cancer, cervical cancer, osteosarcoma.<sup>56,60,69</sup> Another up-miR-124-3p is one of the most highly regulating miRNA and was identified to suppress the metastasis and invasiveness in breast cancer and hepatocellular carcinoma.<sup>72,73</sup> MGAT3 was also reported as tumor suppressor and hepatocellular carcinoma. MGAT3 deficient tumor cells were associated with poor survival rate and prognosis. Higher expression of MGAT3 has been related to poor prognosis in ovarian and cervical cancer as well as colorectal cancer.<sup>38,74,47</sup> MGAT3 has also been reported to inhibit tumor metastasis by targeting growth signaling pathway, EMT pathway.<sup>75,76</sup> Apart from cancer pathways, aberrant regulation of MGAT3 has also been associated with Alzheimer's disease. miRFluR assay data indicate the possibility of miRNAs having much larger role in regulation of MGAT3 specially through upregulation. The study of miRNA mediated upregulation may help us to control the dysregulation of MGAT3 in certain disease types.

Glycosylation enzymes play key role in many cellular functions. But they are often underrepresented due to their complex structure and low expression. Through our work, we have shown that miRNAs can modulate the expression of MGAT3 in both directions. This new mechanism of miRNA regulation can be very significant for genes like MGAT3 that need a very tight regulatory control to not disrupt the cell homeostasis. On the other hand, by mapping a complete miRNA-mRNA interactome for MGAT3 will help us to leverage the use of miRNAs as proxy and decode the underlying mechanism of MGAT3 regulation in disease pathways.

## References

- (1) Lee, R. C.; Feinbaum, R. L.; Ambros, V. The C. Elegans Heterochronic Gene Lin-4 Encodes Small RNAs with Antisense Complementarity to *lin-14*. *Cell* **1993**, *75*, 843–854.
- (2) Wightman, B.; Ha, L.; Ruvkun, G. Posttranscriptional Regulation of the Heterochronic Gene Lin-14 by W-4 Mediates Temporal Pattern Formation in C. Elegans. **1993**, *75*, 855–862.
- (3) Pasquinelli, A. E.; Reinhart, B. J.; Slack, F.; Martindale, M. Q.; Kuroda, M. I.; Maller, B.; Hayward, D. C.; Ball, E. E.; Degan, B.; Müller, P.; et al. Conservation of the Sequence and Temporal Expression of Let-7 Heterochronic Regulatory RNA. *Nat. 2000 4086808* **2000**, *408* (6808), 86–89. <https://doi.org/10.1038/35040556>.
- (4) Kozomara, A.; Birgaoanu, M.; Griffiths-Jones, S. MiRBase: From MicroRNA Sequences to Function. *Nucleic Acids Res.* **2018**, *47*, 155–162. <https://doi.org/10.1093/nar/gky1141>.
- (5) Thu, C. T.; Chung, J. Y.; Dhawan, D.; Vaiana, C. A.; Mahal, L. K. High-Throughput MiRFluR Platform Identifies MiRNA Regulating B3GLCT That Predict Peters' plus Syndrome Phenotype, Supporting the MiRNA Proxy Hypothesis. *ACS Chem. Biol.* **2021**, *16* (10), 1900–1907. [https://doi.org/10.1021/ACSCHEMBIO.1C00247/SUPPL\\_FILE/CB1C00247\\_SI\\_002.XLSX](https://doi.org/10.1021/ACSCHEMBIO.1C00247/SUPPL_FILE/CB1C00247_SI_002.XLSX).
- (6) Diener, C.; Keller, A.; Meese, E. Emerging Concepts of MiRNA Therapeutics: From Cells to Clinic. *Trends Genet.* **2022**, *38* (6), 613–626. <https://doi.org/10.1016/J.TIG.2022.02.006>.
- (7) Li, Z.; Rana, T. M. Therapeutic Targeting of MicroRNAs: Current Status and Future Challenges. *Nat. Rev. Drug Discov.* **2014**, *13* (8), 622–638. <https://doi.org/10.1038/nrd4359>.
- (8) Treiber, T.; Treiber, N.; Meister, G. Regulation of MicroRNA Biogenesis and Its Crosstalk with Other Cellular Pathways. *Nat. Rev. Mol. Cell Biol.* **2019**, *20* (1), 5–20. <https://doi.org/10.1038/s41580-018-0059-1>.
- (9) Petersen, C. P.; Bordeleau, M. E.; Pelletier, J.; Sharp, P. A. Short RNAs Repress Translation after Initiation in Mammalian Cells. *Mol. Cell* **2006**, *21* (4), 533–542. <https://doi.org/10.1016/j.molcel.2006.01.031>.
- (10) Bagga, S.; Bracht, J.; Hunter, S.; Massirer, K.; Holtz, J.; Eachus, R.; Pasquinelli, A. E. Regulation by Let-7 and Lin-4 MiRNAs Results in Target mRNA Degradation. *Cell* **2005**, *122* (4), 553–563. <https://doi.org/10.1016/j.cell.2005.07.031>.
- (11) Liu, J.; Rivas, F. V.; Wohlschlegel, J.; Yates Iii, J. R.; Parker, R.; Hannon, G. J. A Role for the P-Body Component GW182 in MicroRNA Function. *Nat. Cell Biol.* **2005**, *7*. <https://doi.org/10.1038/ncb1333>.
- (12) Pillai, R. S.; Bhattacharyya, S. N.; Artus, C. G.; Zoller, T.; Cougot, N.; Basyuk, E.; Bertrand, E.; Filipowicz, W. Molecular Biology: Inhibition of Translational Initiation by Let-7 MicroRNA in Human Cells. *Science (80-. )*. **2005**, *309* (5740), 1573–1576. [https://doi.org/10.1126/SCIENCE.1115079/SUPPL\\_FILE/PILLAI.SOM.REV](https://doi.org/10.1126/SCIENCE.1115079/SUPPL_FILE/PILLAI.SOM.REV)

1.PDF.

- (13) Vasudevan, S.; Steitz, J. A. AU-Rich-Element-Mediated Upregulation of Translation by FXR1 and Argonaute 2. *Cell* **2007**, *128* (6), 1105–1118. <https://doi.org/10.1016/J.CELL.2007.01.038>.
- (14) Bukhari, S. I. A.; Truesdell, S. S.; Lee, S.; Kollu, S.; Classon, A.; Boukhali, M.; Jain, E.; Mortensen, R. D.; Yanagiya, A.; Sadreyev, R. I.; et al. A Specialized Mechanism of Translation Mediated by FXR1a-Associated MicroRNP in Cellular Quiescence. *Mol. Cell* **2016**, *61* (5), 760–773. <https://doi.org/10.1016/j.molcel.2016.02.013>.
- (15) Zhang, X.; Zuo, X.; Yang, B.; Li, Z.; Xue, Y.; Zhou, Y.; Huang, J.; Zhao, X.; Zhou, J.; Yan, Y.; et al. MicroRNA Directly Enhances Mitochondrial Translation during Muscle Differentiation. *Cell* **2014**, *158* (3), 607–619. <https://doi.org/10.1016/j.cell.2014.05.047>.
- (16) Jame-Chenarboo, F.; Ng, H. H.; Macdonald, D.; Mahal, L. K. High-Throughput Analysis Reveals MiRNA Upregulating  $\alpha$ -2,6-Sialic Acid through Direct MiRNA–mRNA Interactions. *ACS Cent. Sci.* **2022**. <https://doi.org/10.1021/ACSCENTSCI.2C00748>.
- (17) Bartel, D. P. MicroRNAs: Genomics, Biogenesis, Mechanism, and Function. *Cell* **2004**, *116* (2), 281–297. [https://doi.org/10.1016/S0092-8674\(04\)00045-5](https://doi.org/10.1016/S0092-8674(04)00045-5).
- (18) Elkayam, E.; Kuhn, C. D.; Tocilj, A.; Haase, A. D.; Greene, E. M.; Hannon, G. J.; Joshua-Tor, L. The Structure of Human Argonaute-2 in Complex with MiR-20a. *Cell* **2012**, *150* (1), 233. <https://doi.org/10.1016/j.cell.2012.06.021>.
- (19) Vella, M. C.; Choi, E. Y.; Lin, S. Y.; Reinert, K.; Slack, F. J. The C. Elegans MicroRNA Let-7 Binds to Imperfect Let-7 Complementary Sites from the Lin-41 3'UTR. *Genes Dev.* **2004**, *18* (2), 132–137. <https://doi.org/10.1101/GAD.1165404>.
- (20) Brennecke, J.; Stark, A.; Russell, R. B.; Cohen, S. M. Principles of MicroRNA-Target Recognition. <https://doi.org/10.1371/journal.pbio.0030085>.
- (21) Shin, C.; Nam, J. W.; Farh, K. K. H.; Chiang, H. R.; Shkumatava, A.; Bartel, D. P. Expanding the MicroRNA Targeting Code: Functional Sites with Centered Pairing. *Mol. Cell* **2010**, *38* (6), 789–802. <https://doi.org/10.1016/j.molcel.2010.06.005>.
- (22) Lal, A.; Navarro, F.; Maher, C. A.; Maliszewski, L. E.; Yan, N.; O'Day, E.; Chowdhury, D.; Dykxhoorn, D. M.; Tsai, P.; Hofmann, O.; et al. MiR-24 Inhibits Cell Proliferation by Targeting E2F2, MYC, and Other Cell-Cycle Genes via Binding to “Seedless” 3'UTR MicroRNA Recognition Elements. *Mol. Cell* **2009**, *35* (5), 610–625. <https://doi.org/10.1016/j.molcel.2009.08.020>.
- (23) Didiano, D.; Hobert, O. Perfect Seed Pairing Is Not a Generally Reliable Predictor for MiRNA-Target Interactions. **2006**. <https://doi.org/10.1038/nsmb1138>.
- (24) Lee, T.; Wang, N.; Houel, S.; Coutts, K.; Old, W.; Ahn, N. Dosage and Temporal Thresholds in MicroRNA Proteomics. *Mol. Cell. Proteomics* **2015**, *14* (2), 289. <https://doi.org/10.1074/MCP.M114.043851>.
- (25) Wolter, J. M.; Kotagama, K.; Pierre-Bez, A. C.; Firago, M.; Mangone, M. 3'LIFE: A Functional Assay to Detect MiRNA Targets in High-Throughput. *Nucleic Acids Res.* **2014**, *42* (17). <https://doi.org/10.1093/NAR/GKU626>.

- (26) Hsu, S. Da; Lin, F. M.; Wu, W. Y.; Liang, C.; Huang, W. C.; Chan, W. L.; Tsai, W. T.; Chen, G. Z.; Lee, C. J.; Chiu, C. M.; et al. MiRTarBase: A Database Curates Experimentally Validated MicroRNA-Target Interactions. *Nucleic Acids Res.* **2011**, *39* (Database issue). <https://doi.org/10.1093/NAR/GKQ1107>.
- (27) Ohtsubo, K.; Marth, J. D. Glycosylation in Cellular Mechanisms of Health and Disease. *Cell* **2006**, *126* (5), 855–867. <https://doi.org/10.1016/J.CELL.2006.08.019>.
- (28) H Smith, B. A.; Bertozzi, C. R. The Clinical Impact of Glycobiology: Targeting Selectins, Siglecs and Mammalian Glycans. *Nat. Rev. Drug Discov.* <https://doi.org/10.1038/s41573-020-00093-1>.
- (29) Jaeken, J. Congenital Disorders of Glycosylation. *Ann. N. Y. Acad. Sci.* **2010**, *1214* (1), 190–198. <https://doi.org/10.1111/J.1749-6632.2010.05840.X/PDF>.
- (30) Lebrilla, C. B.; Liu, J.; Widmalm, G.; Prestegard, J. H. Oligosaccharides and Polysaccharides. *Essentials Glycobiol.* **2022**. <https://doi.org/10.1101/GLYCOBIOLOGY.4E.3>.
- (31) Reily, C.; Stewart, T. J.; Renfrow, M. B.; Novak, J. Glycosylation in Health and Disease. <https://doi.org/10.1038/s41581-019-0129-4>.
- (32) Colley, K. J.; Varki, A.; Haltiwanger, R. S.; Kinoshita, T. Cellular Organization of Glycosylation. *Essentials Glycobiol.* **2022**. <https://doi.org/10.1101/GLYCOBIOLOGY.4E.4>.
- (33) Schjoldager, K. T.; Narimatsu, Y.; Joshi, H. J.; Clausen, H. Global View of Human Protein Glycosylation Pathways and Functions. *Nat. Rev. Mol. Cell Biol.* <https://doi.org/10.1038/s41580-020-00294-x>.
- (34) Helenius, A.; Aebi, M. Intracellular Functions of N-Linked Glycans. *Science* (80-. ). **2001**, *291* (5512), 2364–2369. <https://doi.org/10.1126/SCIENCE.291.5512.2364>.
- (35) Chen, Q.; Tan, Z.; Guan, F.; Ren, Y. The Essential Functions and Detection of Bisecting GlcNAc in Cell Biology. *Front. Chem.* **2020**, *8*, 511. <https://doi.org/10.3389/FCHEM.2020.00511/BIBTEX>.
- (36) Zhang, M.; Wang, M.; Gao, R.; Liu, X.; Chen, X.; Geng, Y.; Ding, Y.; Wang, Y.; He, J. Altered B1,6-GlcNAc and Bisecting GlcNAc-Branched N-Glycan on Integrin B1 Are Associated with Early Spontaneous Miscarriage in Humans. *Hum. Reprod.* **2015**, *30* (9), 2064–2075. <https://doi.org/10.1093/HUMREP/DEV153>.
- (37) Gu, J.; Isaji, T.; Xu, Q.; Kariya, Y.; Gu, W.; Fukuda, T.; Du, Y. Potential Roles of N-Glycosylation in Cell Adhesion. *Glycoconj. J.* **2012**, *29* (8–9), 599–607. <https://doi.org/10.1007/S10719-012-9386-1/FIGURES/4>.
- (38) Kohler, R. S.; Anugraham, M.; López, M. N.; Xiao, C.; Schoetzau, A.; Hettich, T.; Schlotterbeck, G.; Fedier, A.; Jacob, F.; Heinzelmann-Schwarz, V. Epigenetic Activation of MGAT3 and Corresponding Bisecting GlcNAc Shortens the Survival of Cancer Patients. *Oncotarget* **2016**, *7* (32), 51674–51686. <https://doi.org/10.18632/ONCOTARGET.10543>.
- (39) Nakano, M.; Mishra, S. K.; Tokoro, Y.; Sato, K.; Nakajima, K.; Yamaguchi, Y.; Taniguchi, N.; Kizuka, Y. Bisecting GlcNAc Is a General Suppressor of Terminal Modification of N-Glycan. *Mol. Cell. Proteomics* **2019**, *18* (10),

- 2044–2057. <https://doi.org/10.1074/mcp.RA119.001534>.
- (40) Wang, M.; Zhu, J.; Lubman, D. M.; Gao, C. Aberrant Glycosylation and Cancer Biomarker Discovery: A Promising and Thorny Journey HHS Public Access. *Clin Chem Lab Med* **2019**, *57* (4), 407–416. <https://doi.org/10.1515/cclm-2018-0379>.
- (41) Kurcon, T.; Liu, Z.; Paradkar, A. V.; Vaiana, C. A.; Koppolu, S.; Agrawal, P.; Mahal, L. K. MiRNA Proxy Approach Reveals Hidden Functions of Glycosylation. *Proc. Natl. Acad. Sci. U. S. A.* **2015**, *112* (23), 7327–7332. [https://doi.org/10.1073/PNAS.1502076112/SUPPL\\_FILE/PNAS.1502076112.SD01.XLSX](https://doi.org/10.1073/PNAS.1502076112/SUPPL_FILE/PNAS.1502076112.SD01.XLSX).
- (42) Agrawal, P.; Kurcon, T.; Pilobello, K. T.; Rakus, J. F.; Koppolu, S.; Liu, Z.; Batista, B. S.; Eng, W. S.; Hsu, K. L.; Liang, Y.; et al. Mapping Posttranscriptional Regulation of the Human Glycome Uncovers MicroRNA Defining the Glycocode. *Proc. Natl. Acad. Sci. U. S. A.* **2014**, *111* (11), 4338–4343. [https://doi.org/10.1073/PNAS.1321524111/SUPPL\\_FILE/SAPP.PDF](https://doi.org/10.1073/PNAS.1321524111/SUPPL_FILE/SAPP.PDF).
- (43) Johnson, J. M.; Castle, J.; Garrett-Engele, P.; Kan, Z.; Loerch, P. M.; Armour, C. D.; Santos, R.; Schadt, E. E.; Stoughton, R.; Shoemaker, D. D. Genome-Wide Survey of Human Alternative Pre-mRNA Splicing with Exon Junction Microarrays. *Science (80-. )*. **2003**, *302* (5653), 2141–2144. <https://doi.org/10.1126/SCIENCE.1090100>.
- (44) Mariella, E.; Marotta, F.; Grassi, E.; Gilotto, S.; Provero, P. The Length of the Expressed 3' UTR Is an Intermediate Molecular Phenotype Linking Genetic Variants to Complex Diseases. *Front. Genet.* **2019**, *10* (JUL), 714. <https://doi.org/10.3389/FGENE.2019.00714/BIBTEX>.
- (45) Fagerberg, L.; Hallstrom, B. M.; Oksvold, P.; Kampf, C.; Djureinovic, D.; Odeberg, J.; Habuka, M.; Tahmasebpour, S.; Danielsson, A.; Edlund, K.; et al. Analysis of the Human Tissue-Specific Expression by Genome-Wide Integration of Transcriptomics and Antibody-Based Proteomics \*. *Mol. Cell. Proteomics* **2014**, *13* (2), 397–406.
- (46) Sjöstedt, E.; Zhong, W.; Fagerberg, L.; Karlsson, M.; Mitsios, N.; Adori, C.; Oksvold, P.; Edfors, F.; Limiszewska, A.; Hikmet, F.; et al. An Atlas of the Protein-Coding Genes in the Human, Pig, and Mouse Brain. *Science (80-. )*. **2020**, *367* (6482). <https://doi.org/10.1126/SCIENCE.AAY4106>.
- (47) Huang, H.; Liu, Y.; Yu, P.; Qu, J.; Guo, Y.; Li, W.; Wang, S.; Zhang, J. MiR-23a Transcriptional Activated by Runx2 Increases Metastatic Potential of Mouse Hepatoma Cell via Directly Targeting Mgat3. *Sci. Rep.* **2018**, *8* (1). <https://doi.org/10.1038/S41598-018-25768-Z>.
- (48) Gupta, R.; Leon, F.; Thompson, C. M.; Nimmakayala, R.; Karmakar, S.; Nallasamy, P.; Chugh, S.; Prajapati, D. R.; Rachagani, S.; Kumar, S.; et al. Global Analysis of Human Glycosyltransferases Reveals Novel Targets for Pancreatic Cancer Pathogenesis. *Br. J. Cancer* **2020**, *122* (11), 1661–1672. <https://doi.org/10.1038/s41416-020-0772-3>.
- (49) Krüger, J.; Rehmsmeier, M. RNAhybrid: MicroRNA Target Prediction Easy, Fast and Flexible. *Nucleic Acids Res.* **2006**, *34* (suppl\_2), W451–W454. <https://doi.org/10.1093/NAR/GKL243>.
- (50) Niu, H.; Qu, A.; Guan, C. Suppression of MGAT3 Expression and the

- Epithelial–Mesenchymal Transition of Lung Cancer Cells by MiR-188-5p. *Biomed. J.* **2021**, *44* (6), 678–685. <https://doi.org/10.1016/J.BJ.2020.05.010>.
- (51) Kizuka, Y.; Taniguchi, N. Enzymes for N-Glycan Branching and Their Genetic and Nongenetic Regulation in Cancer. *Biomol. 2016, Vol. 6, Page 25* **2016**, *6* (2), 25. <https://doi.org/10.3390/BIOM6020025>.
- (52) Granovsky, M.; Fata, J.; Pawling, J.; Muller, W. J.; Khokha, R.; Dennis, J. W. Suppression of Tumor Growth and Metastasis in Mgat5-Deficient Mice. *Nat. Med.* **2000**, *6* (3), 306–312. <https://doi.org/10.1038/73163>.
- (53) Xu, J.; Zheng, J.; Wang, J.; Shao, J. MiR-876-5p Suppresses Breast Cancer Progression through Targeting TFAP2A. *Exp. Ther. Med.* **2019**, *18* (2), 1458–1464. <https://doi.org/10.3892/ETM.2019.7689>.
- (54) Wang, Y.; Xie, Y.; Li, X.; Lin, J.; Zhang, S.; Li, Z.; Huo, L.; Gong, R. MiR-876-5p Acts as an Inhibitor in Hepatocellular Carcinoma Progression by Targeting DNMT3A. *Pathol. - Res. Pract.* **2018**, *214* (7), 1024–1030. <https://doi.org/10.1016/J.PRP.2018.04.012>.
- (55) Biamonte, F.; Santamaria, G.; Sacco, A.; Perrone, F. M.; Di Cello, A.; Battaglia, A. M.; Salatino, A.; Di Vito, A.; Aversa, I.; Venturella, R.; et al. MicroRNA Let-7g Acts as Tumor Suppressor and Predictive Biomarker for Chemoresistance in Human Epithelial Ovarian Cancer. *Sci. Reports 2019 91* **2019**, *9* (1), 1–12. <https://doi.org/10.1038/s41598-019-42221-x>.
- (56) Wang, Y.; Li, Y.; Wu, B.; Shi, C.; Li, C. MicroRNA-661 Promotes Non-Small Cell Lung Cancer Progression by Directly Targeting RUNX3. *Mol. Med. Rep.* **2017**, *16* (2), 2113–2120. <https://doi.org/10.3892/MMR.2017.6827>.
- (57) Hoffman, Y.; Bublik, D. R.; Pilpel, Y.; Oren, M. MiR-661 Downregulates Both Mdm2 and Mdm4 to Activate P53. *Cell Death Differ.* *2014 212* **2013**, *21* (2), 302–309. <https://doi.org/10.1038/cdd.2013.146>.
- (58) Wang, Y.; Chen, A.; Zheng, C.; Zhao, L. MiR-92a Promotes Cervical Cancer Cell Proliferation, Invasion, and Migration by Directly Targeting PIK3R1. *J. Clin. Lab. Anal.* **2021**, *35* (8), e23893. <https://doi.org/10.1002/JCLA.23893>.
- (59) Cao, S.; Jiang, L.; Shen, L.; Xiong, Z. Role of MicroRNA-92a in Metastasis of Osteosarcoma Cells in Vivo and in Vitro by Inhibiting Expression of TCF21 with the Transmission of Bone Marrow Derived Mesenchymal Stem Cells. *Cancer Cell Int.* **2019**, *19* (1), 1–17. <https://doi.org/10.1186/S12935-019-0741-1/TABLES/3>.
- (60) Huang, Y. F.; Liu, M. W.; Xia, H. B.; He, R. Expression of MiR-92a Is Associated with the Prognosis in Non-Small Cell Lung Cancer: An Observation Study. *Med. (United States)* **2022**, *101* (41), E30970. <https://doi.org/10.1097/MD.00000000000030970>.
- (61) Zhang, X.; Wang, X.; Chai, B.; Wu, Z.; Liu, X.; Zou, H.; Hua, Z.; Ma, Z.; Wang, W. Downregulated MiR-18a and MiR-92a Synergistically Suppress Non-Small Cell Lung Cancer via Targeting Sprouty 4. *Bioengineered* **2022**, *13* (4), 11281–11295. [https://doi.org/10.1080/21655979.2022.2066755/SUPPL\\_FILE/KBIE\\_A\\_2066755\\_SM8987.DOCX](https://doi.org/10.1080/21655979.2022.2066755/SUPPL_FILE/KBIE_A_2066755_SM8987.DOCX).
- (62) Kiener, M.; Chen, L.; Krebs, M.; Grosjean, J.; Klima, I.; Kalogirou, C.; Riedmiller, H.; Kneitz, B.; Thalmann, G. N.; Snaar-Jagalska, E.; et al. MiR-

- 221-5p Regulates Proliferation and Migration in Human Prostate Cancer Cells and Reduces Tumor Growth in Vivo. *BMC Cancer* **2019**, *19* (1), 1–17. <https://doi.org/10.1186/S12885-019-5819-6/FIGURES/5>.
- (63) Su, A.; He, S.; Tian, B.; Hu, W.; Zhang, Z. MicroRNA-221 Mediates the Effects of PDGF-BB on Migration, Proliferation, and the Epithelial-Mesenchymal Transition in Pancreatic Cancer Cells. *PLoS One* **2013**, *8* (8), e71309. <https://doi.org/10.1371/JOURNAL.PONE.0071309>.
- (64) Uhlén, M.; Fagerberg, L.; Hallström, B. M.; Lindskog, C.; Oksvold, P.; Mardinoglu, A.; Sivertsson, Å.; Kampf, C.; Sjöstedt, E.; Asplund, A.; et al. Tissue-Based Map of the Human Proteome. *Science* (80-. ). **2015**. <https://doi.org/10.1126/SCIENCE.1260419>.
- (65) Kosti, I.; Jain, N.; Aran, D.; Butte, A. J.; Sirota, M. Cross-Tissue Analysis of Gene and Protein Expression in Normal and Cancer Tissues OPEN. **2016**. <https://doi.org/10.1038/srep24799>.
- (66) Vogel, C.; Marcotte, E. M. Insights into the Regulation of Protein Abundance from Proteomic and Transcriptomic Analyses. *Nat. Rev. Genet.* *2012* **13** (4), 227–232. <https://doi.org/10.1038/nrg3185>.
- (67) Baek, D.; Villén, J.; Shin, C.; Camargo, F. D.; Gygi, S. P.; Bartel, D. P. The Impact of MicroRNAs on Protein Output. *Nat.* *2008* **455** (7209), 64–71. <https://doi.org/10.1038/nature07242>.
- (68) Nagae, M.; Soga, K.; Morita-Matsumoto, K.; Hanashima, S.; Ikeda, A.; Yamamoto, K.; Yamaguchi, Y. Phytohemagglutinin from Phaseolus Vulgaris (PHA-E) Displays a Novel Glycan Recognition Mode Using a Common Legume Lectin Fold. *Glycobiology* **2014**, *24* (4), 368–378. <https://doi.org/10.1093/GLYCOB/CWU004>.
- (69) Patnaik, S. K.; Kannisto, E.; Mallick, R.; Yendamuri, S. Overexpression of the Lung Cancer-Prognostic MiR-146b MicroRNAs Has a Minimal and Negative Effect on the Malignant Phenotype of A549 Lung Cancer Cells. <https://doi.org/10.1371/journal.pone.0022379>.
- (70) Jiang, M.; Li, X.; Quan, X.; Li, X.; Zhou, B. MiR-92a Family: A Novel Diagnostic Biomarker and Potential Therapeutic Target in Human Cancers. *Front. Mol. Biosci.* **2019**, *6*, 98. <https://doi.org/10.3389/FMOLB.2019.00098/BIBTEX>.
- (71) Zhou, P.; Xu, W.; Peng, X.; Luo, Z.; Xing, Q.; Chen, X.; Hou, C.; Liang, W.; Zhou, J.; Wu, X.; et al. Large-Scale Screens of MiRNA-MRNA Interactions Unveiled That the 3'UTR of a Gene Is Targeted by Multiple MiRNAs. *PLoS One* **2013**, *8* (7), e68204. <https://doi.org/10.1371/JOURNAL.PONE.0068204>.
- (72) Wang, Y.; Chen, L.; Wu, Z.; Wang, M.; Jin, F.; Wang, N.; Hu, X.; Liu, Z.; Zhang, C. Y.; Zen, K.; et al. MiR-124-3p Functions as a Tumor Suppressor in Breast Cancer by Targeting CBL. *BMC Cancer* **2016**, *16* (1), 1–9. <https://doi.org/10.1186/S12885-016-2862-4/FIGURES/4>.
- (73) Majid, A.; Wang, J.; Nawaz, M.; Abdul, S.; Ayesha, M.; Guo, C.; Liu, Q.; Liu, S.; Sun, M. Z. MiR-124-3p Suppresses the Invasiveness and Metastasis of Hepatocarcinoma Cells via Targeting CRKL. *Front. Mol. Biosci.* **2020**, *7*, 223. <https://doi.org/10.3389/FMOLB.2020.00223/BIBTEX>.
- (74) Allam, H.; Johnson, B. P.; Zhang, M.; Lu, Z.; Cannon, M. J.; Abbott, K. L. The

Glycosyltransferase GnT-III Activates Notch Signaling and Drives Stem Cell Expansion to Promote the Growth and Invasion of Ovarian Cancer. *J. Biol. Chem.* **2017**, 292 (39), 16351–16359.

<https://doi.org/10.1074/JBC.M117.783936>.

- (75) Song, Y.; Aglipay, J. A.; Bernstein, J. D.; Goswami, S.; Stanley, P. The Bisecting GlcNAc on N-Glycans Inhibits Growth Factor Signaling and Retards Mammary Tumor Progression. *Cancer Res.* **2010**, 70 (8), 3361–3371.  
<https://doi.org/10.1158/0008-5472.CAN-09-2719>.
- (76) Pucci, M.; Malagolini, N.; Dall'Olio, F. Glycobiology of the Epithelial to Mesenchymal Transition. *Biomed. 2021, Vol. 9, Page 770* **2021**, 9 (7), 770.  
<https://doi.org/10.3390/BIOMEDICINES9070770>.

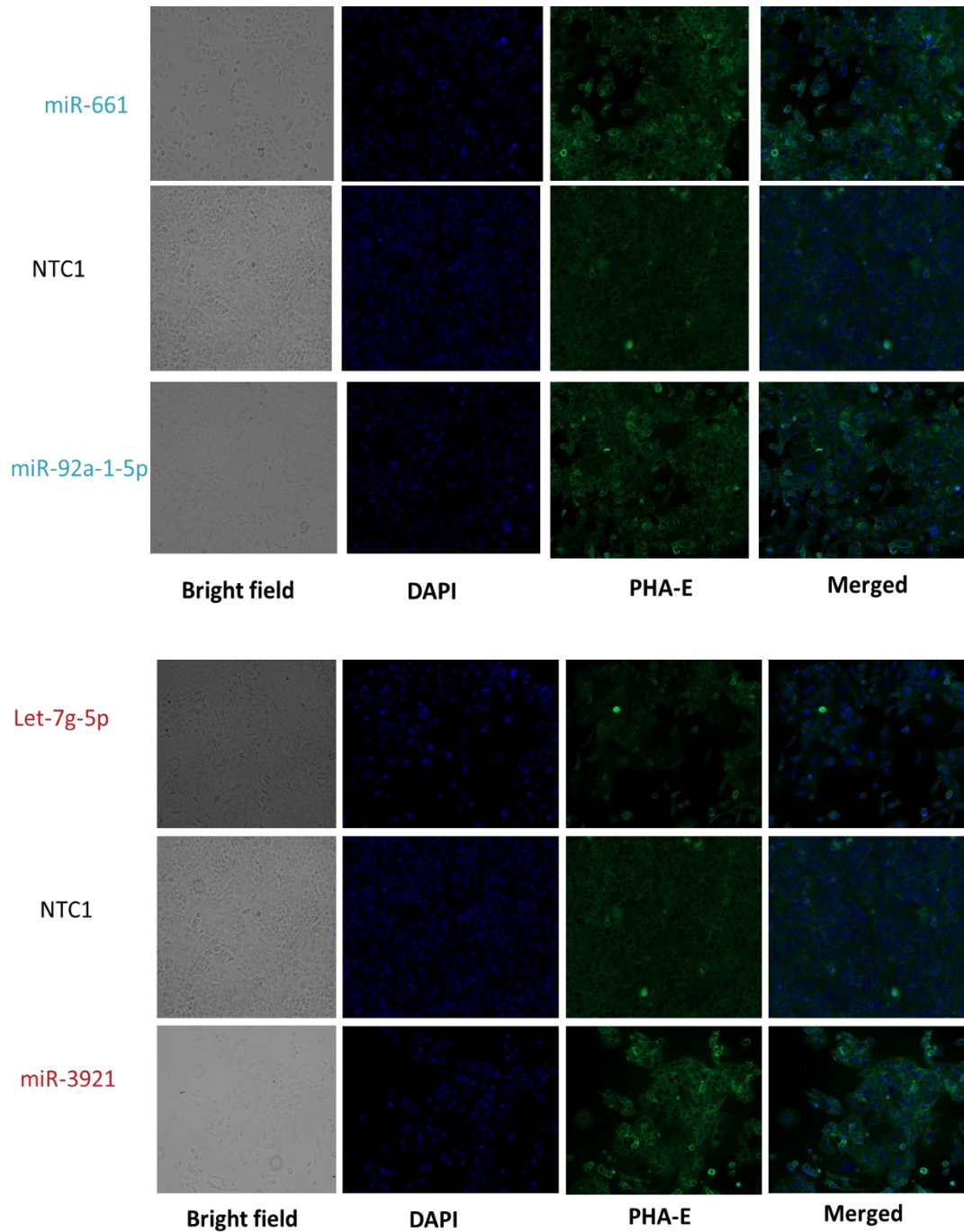
## Appendix-1. 3'UTR sequence of MGAT3

AGCTGCATGATCTGATAGGGTTTGTGACAGGGCGGGGGTGGCGGGGCCCTAGCGCTATCTCCCTGCCTCCTGCC  
GGCTCCTTGGTTCTTGAGGGGACCAGGAGTGGGTGGGGAGTGGGGGTAGGGTTTCCCTACTGAAGCCCT  
TGTGAATCAAGGGTCAGGCCTTTGAGCTCAGAAAATATCCCTCCTGTTGGGAGAGGGCGCAGGCCGTGACGTCTG  
GGTGGCCCTTACTGCCAAGACTGCTGTGGCCAGGAGGTGCCACTGGAGTGTGCGTGGTGGTCCCTGGGTAGC  
GGGGAGGGTAGGCAGGATTGGGGAAGAGAGCCTGCAGGATCTCACCAGGCAGCCTCTGGGGGTGGCCAGGCC  
GGAAAAAGCCACCATTGGCATCCCTGGGCCTTGGCTCCGTGTGGGAGACCGGCTGCCAGGAGGCCAGG  
GCTCTGTAAGTAGATGCATTTGGGTCCAGGAGGAAGCGTGGACACCTCGTAGGGAAGAGATGAAAAAGCCACAT  
CCTACCAAGAGGAGGTGCTGAGGGATGCTTTCAGTGTAGTCAAGAAGTGTGGCCAGATGGAGACAGAACTCC  
ACCCCTGCCGCAAAGGACAGGACCTGGCTGCCCTGGGATGCTGGTGCCTGAGTCTGTCTCTGTGACCCCTCAGG  
CTGCTGTGACCAACACAGGGGCCTGGAGAACCCTGAGGAGCTTTCCTTTGGTTCTAAACCCGGCGTTGACGTTT  
TTCTCCATTACATTGCTGTCTTGTGGACTGTGCACTCAGTCCCTGCAAGGCCAAGAGTCCAGTTGTAGGTGTGG  
CCTTGAGGGGAAGTGGGGAGGAGAAGACTGACATGAGTCTCTGCACGGATCCGTCTCTCCCTCCCCATCACC  
CTTCTTCTGACACCCAGTCCAGCTGTCCACTGTCCAGGTGCAGTCACTGTTGTGCCCTTCTTGGGGCAGGCTG  
GCTGGGGGCCAGAAAGGGGCCATGAGGCTGTCTGGGCCCCAAAAGGGACAATAAGGCCAGTTGTATGCTTCCTG  
TTCTCATAGCTTGCCTTGGTGGGGATGTCTTTGTTGGAGTTGATTCTGAGCTGCTGTGATTAGGAGACCCTGAAA  
TACAGTGGTTTAAAGCAAGATGGAAGCTTGTCTTAATTAGTCTAGATTGAGATGGCCCAGAGCTGGTAGGGCAGC  
TCTGCGTTTCTTCATACGCACCTTCCAATTCTGGGTACACAGCGGCTGCTCCAGCGCCACCCTCCTGTGTGCATCC  
AAGCTGGGGGAAGCAGAAATAGACAAGAGGGCACACCCACTTTTTGCTAAAGGCATGAGCCAGAATTGGCAGG  
CTCACCTCTGCTGGCCTCTCATTGGCTGGGACTCAGTCACATGGCCACAAGCAGCTGCTAGGGAACCTGGGAAGT  
GTAGTCTTACAGCGGGCCGCCATGTGCCTGGCCTCACCTTGGGAGTTATCTTATTGATGGAGGAGAAGAGAATGG  
ATATGGGGGACCAGTAGCATCTCTGGGAGAGGGGGAGGGAGCAGCAATAACTCAGTCGTCGGATCCAGCTCTCAT  
TGTCAGAGTTTCCGGAACAGCTTGTCTCTGTTCCCTCACTGTGCAGCCAGGGCTGGGGGCAGTGAGGAGCTTGG  
AGCTGTGGGAAGGGGAAACACCCCTCCCTCGGCCCTCAGACGCTACCAATGATGCCGTTTGCAGAGTT  
GGCCTGGAATGGCTCATGTTTGTGCGTGTGTGTGTATATTTATGGGCATGGGTGCATGCTTGGTGTGATTTTG  
TACATGTCTGTATTGCTGTGTCCCTGTAATAACATGCTTGTGTATGGATGGAAGAGGCCAGGCCAGGCCTGGCCT  
CTTCTCGGGCCTGTGGCCACACCTCCTGCAGCTCCCCAAAATGACTGAGGCAGAAAGCCCTTGGGGAGCCTAGA  
AAGCAAAGCTAAAGGGGATGCAGGGTCTGTCTGTCTGTCTTTCAGTCTGAGGAATGAGAATCCTGACCTGA  
GGGCTGTGCAGCTGAGAGCCCACTACCTCCCCAGCCCTCTCGGCCCCAGCCGCATCATCCCACCTGTCCCTCCC  
CCCCACCTCCAGTGGGGCTTTCTCCAGATGTCTTATGGTTGGGGGTTTCTGATGGGCCAGGAGAGGGGCATCT  
TCTTGCGACAGCACTGTCTGGGTTAAGTGCCAGTGAGGGCATGGTGTGGGGAGCTGGCCTCAGAGGAGCCGCTG  
GTGGCAAGCGTGAAGTGGGCTGAGGGGCTCTGAGCCACTTTGCTCCCATCTAGGGGACTGCCCCCATGGAAT  
CCTTTGAAGTCACAGCAGCCTTCTTCTGTTTGTCTTGGGGCTGAGAGGTGGCTCAAACACTCGGGGTCCCTAT  
GGCTCTGGGTCAATCTAGGCCAGGCTGCACCCCATGGACAGGGAGTCTCAGGGCTCCTGATCATGCCAGGCCCT  
GGCCTGGGGCCTCCCTCCTTGGCAGCTTCCACCCCCACGCCCTGGCATCCTCAGTTGCTATGGGATGCCCTC  
CAGGGCACACAGCTCAGGGCTAAGCGAAGGAAGATAGGAGCAGCTCAGAGCTGCCAGGCTCTGCCTTCTCACAG  
ACCTGTGGGGCAGGTCCTGTTTACAGCAGCAGGAGTGAAGGCCTGGCCATCGGTGGAGAGGGCAGCTGTCAGA  
GGGCTGGGGGCCAGGGCACAGGATTGAAGAGTTTACATATCATCACAGCATACTGGGAATTTGGTGGGGGCA  
GAAGAACCAGGGCCACTCCCTCAATATGAAGGAAACCAAGCTGAATGTGACCACCGGCACACTGCTGCCATGT  
CCCATGTCCACCTTCTCCCCGGGAATAACTGGCCCTGAGACCCCTAGACCCAAGGAGGCCTGTCCATGCCAAGC  
ATCCGGGAAGCATGGCTGGCCTTATCCACCCATGGGTACGTCGGTTCCAGGGGCAGCATGGGAGATCTTTGGG  
GGCAACAGGGAGAGTCTGGGTGGGGAGACGGGACTTGTCCAAGCAGAAGGCAGGACCTGGGAAATGCATAATG  
TAAGGACATCAATAATAGTATTATTTTTTTTGTAAAGGAAAATCAATATGTACATTCTGAAATCATTTTCTGTAA  
ATGGTTGGATTTCATTTACCCCTAAAGGGATGCTTAAAGGAGAAGATAATATTAATAATAAAAAACAGCTACAAA  
GTCTGAA

## Appendix-2. MGAT3-3' UTR mutated sequence

AGCTGCATGATCTGATAGGGTTTGTGACAGGGCGGGGGTGGCGGGCGCCCTAGCGCTATCTCCCTGCCTCCTGCC  
GGTCCTTGGTTCTTGAGGGGACCAGGAGTGGGTGGGGAGTGGGGGTGGGGGTAGGGTTTCCCTACTGAAGCCCT  
TGTGAATCAAGGGTCAGGCCTTTGAGCTCAGAAAATATCCCTCCTGTTGGGAGAGGGCGCAGGCCGTGACGTCTG  
GGTGGCCCTTATGACTGCCAAGACTGCTGTGGCCAGGAGGTGCCACTGGAGTGTGCGTGGTGGTCCCTGGGTAGC  
GGGGGAGGGTAGGCAGGATTGGGGAAGAGAGCCTGCAGGATCTCACCAGGCAGCCTCTGGGGGTGGCCAGGCC  
GGGAAAAGCCACCATTGGCATCCCTGGGCCTTGGGCTCCGTGTGGGAGACCGGCCTGCCAGGAGGACCCAGG  
GCTCTGTAAGTAGATGCATTTGGGTCCAGGAGGAAGCGTGGACACCTCGTAGGGAAGAGATGAAAAAGCCACAT  
CCTACCAAGAGGAGGTGCTGAGGGATGCTTTGCAGTGTAGTCAGAAGTGTGGGCCAGATGGAGACAGAACCTCC  
ACCCCTGCCGCAAAGGACAGGACCTGGCTGCCCTGGGATGCTGGTGCCTGAGTCTGTCTCTGTGCACCCCTCAGG  
CTGTCGTGAGCCAACACAGGGGCTGGAGAACCCTGAGGAGCTTTCCTTTTGGTTCTAAACCCGGCGTTGACGTTT  
CTTCTCCCTTTCACATTGCTGTCTTGTGGACTGTGCACTCAGTCCTTGAAGGCCAAGAGTCCAGTTGTAGGTGTGG  
CCTAGAGGGGGAAGTGGGGAGGAGAAGACTGACATGAGTCCTCTGCACGGATCCGTCCTCCCTCCCCATACCC  
CTTCTTCTGACACCCAGTCCAGCTGTCCACTGTCCAGGTGCAGTCACTGTTGTGCCCTTCTTGGGGCAGGCTG  
GCTGGGGGCCAGAAAGGGGCCATGAGGCTGTCTGGGCCAAAAAGGGACAATAAGGCCAGTTGTATGCTTCCCTG  
TTCTCATAGCTTGCTTGGTGGGGATGTCTTTGTTGGAGTTGATTCTGAGCTGCTGTGATTAGGAGACCCTGAAA  
TACAGTGGTTTAAAGCAAGATGGAAGCTTGTTCCTAATTAGTCTAGATTGAGATGGCCAGAGCTGGTAGGGCAGC  
TCTGCGTTTCTTCATACGCACCTTCCAATTCTGGGTACACAGCGGCTGCTCCAGCGCCACCCTCCTGTGTGCATCC  
AAGCCTGGGGGAAGCAGAAAATAGACAAGAGGGCACACCCACTTTTTGCTAAAGGCATGAGCCAGAATTGGCAGG  
CTCACCTCTGCTGGCCTCTCATTGGCTGGGACTCAGTCACATGGCCACAAGCAGCTGCTAGGGAACTGGGAAAGT  
GTAGTCTTACAGCGGGCCGCCATGTGCCTGGCCTACCTTGGGAGTTATCTTATTGATGGAGGAGAAGAGAATGG  
ATATGGGGGACCAGTAGCATCTCTGGGAGAGGGGGAGGGAGCAGCAATAAATCAGTCGTCGGATCCAGCTCTCAT  
TGTCAGAGTTTCCGGAACAGCTTGTCTCCTGTTTCCCTCACTGTGCAGCCCAGGGCTGGGGGCAGTGAGGAGCTTG  
AGCTCTGTGGGAAGGGGAAAACACCCCTCCCTCGGCCCTCAGACGCTACCCAATGATGCCGTTTGCAGAGTT  
GGCCTGTGGAATGGCTCATGTTTGTGCGTGTGTGTGTATATTTATGGGCATGGGTGCATGCTTGGTGTGTATTTG  
TACATGTCTGTATTGCTGTGTCCCTGTAATAACATGCTTGTGTATGGATGGAAGAGGCCAGGCCAGGCCTGGCCT  
CTTCTCGGGCCTGTGGCCACACCTCCTGCAGCTCCCCAAAATGACTGAGGCAGAAAGCCCTTGGGGAGCCTAGA  
AAGCAAAGCTAAAGGGGATGCAGGGTCTGTCTGTCTGTCTTTTCACTGAGGAATGAGAATCCTGACCTGA  
CTACCTCCCCAGCCCTCTCGGGCCAGCCGATCATCCACCTGTCCCCTCCCCCACCCTCAGTGGGGCTTTTCT  
CCAGATGCTTATGGTTGGGGTTTCTGATGGGCCAGGAGAGGAGGGCATCTTCTTGCAGACACTGTCTGGGT  
TAAGTGCCAGTGAGGGCATGGTGTGGGGAGCTGGCCTCAGAGGAGCCGCTGGTGGGCAAGCGTGAAGTGGGCT  
GAGGGGCTCTGAGCCACTTGTCTCCATCTAGGGGACTGCCCCCATGGAACCTTTGAAGTCACAGCAGCCTTC  
CTTCTGTTTGTCTTGGGGCTGAGAGGTGGCTCAAACACTCGGGGTCCCTATGGCTCTGGGTCAATCTAGGCCAG  
GCTGACCCCATGGACAGGAGTCTCAGGGCTCCTGATGCCAGCCCTGGCCTGGGGCCTCCCTCCTTGGCA  
GCTTTCCACCCCCACGCCCTGGCATCCTCAGTTGCTATGGGATGCCCTCCAGGGCACAGCTCAGGGCTAAGC  
GAAGGAAGATAGGAGCAGCTCAGAGCTGCCAGGCTCTGCCTTCTCACAGACCTGGTGGGGCAGGTCTCTTTCAC  
AGCAGCAGGAGTGAAGGCCTGGCCATCGGTGGAGAGGGCAGCTGTCAGAGGGCTGGGGGCCAGGGCACAGGATT  
GAAGAGTTTACATATCATCACAGCATACTGGGAATTTGGTGGGGGCAAGAAGAACCCAGGGCCACTCCCTCAA  
TATGAAGGGAAAACCAAGCTGAATGTGACCACCGGCACACTGCTGCCATGTCCATGTCCACCTTCTCCCCGGGA  
ATAACTGGCCCTGAGACCCCTAGACCCAAGGAGGCCTGTCCATGCCAAGCATCCGGGAAGCATGGCTGGCCTTAT  
CCACCCATGGGTACGTCGGTTCCAGGGGACAGCATGGGAGATCTTTGGGGGCAACAGGGGAGAGTCTGGGTGGG  
GAGACGGGACTTGTCCAAGCAGAAGGCAGGACCCTGGGAAATGCATAATGTAAGGACATCAATAATAGTATTATT  
TTTTTTGTAAGGGAAAATCAATATGTACATTCTGAAATCATTCTCTGTAAATGGTTGGATTTCATTCACCCCTA  
AAGGGATGCTTAAAGGAGAAGATAATATTAATAATAAAAAACAGCTACAAAAGTCTGA

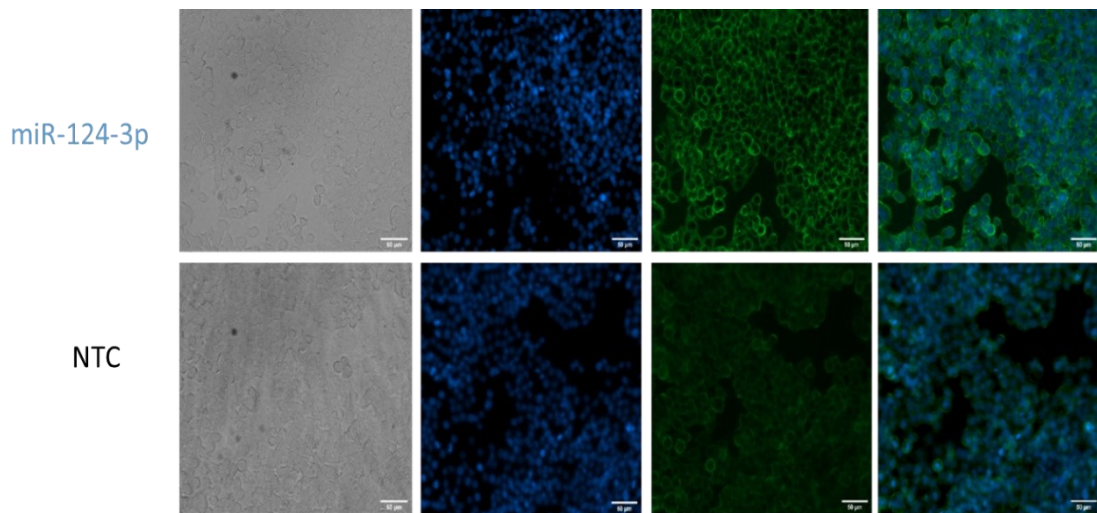
### Appendix-3. PHA-E lectin staining in A549 cell line



PHA-E lectin staining in A549 cell line. Change in bisecting-GlcNAc level is

consistent with miR-mediated up and down regulation of MGAT3. Up-miRs and down-miRs are color coded as blue and red respectively. Cells were treated with PNGaseF enzyme prior to verify the staining of bisecting GlcNAc.

#### Appendix-4. PHA-E lectin staining in HT29



**PHA-E lectin staining in HT29.** Change in bisecting-GlcNAc level is consistent with miR-mediated up and down-regulation of MGAT3. Up-miRs and down-miRs are color-coded as blue and red respectively. Cells were treated with PNGaseF enzyme prior to verify the staining of bisecting GlcNAc.

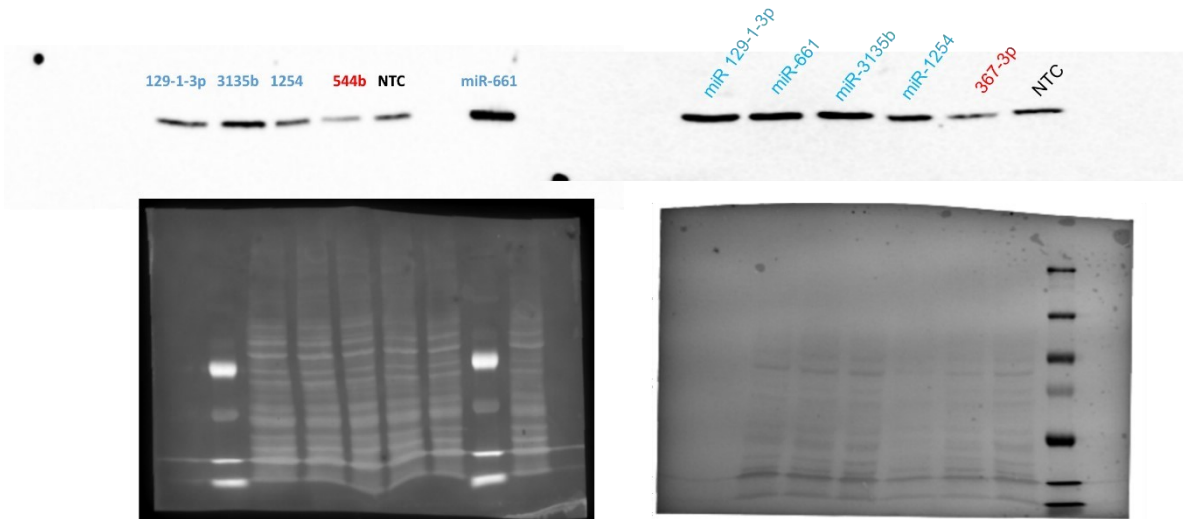
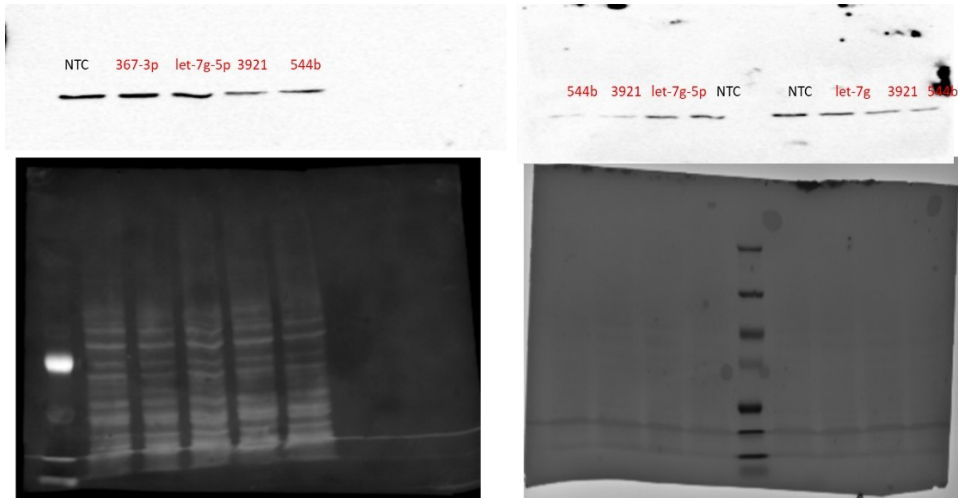
**Appendix-5: List of miRNA hits for MGAT3 in the miRFluR assay**

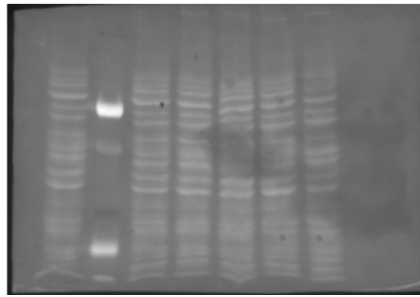
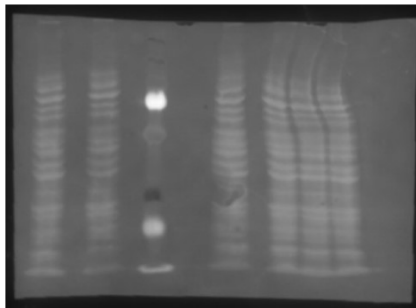
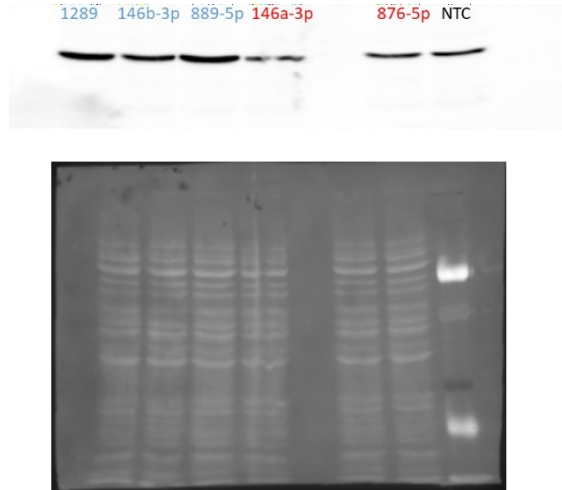
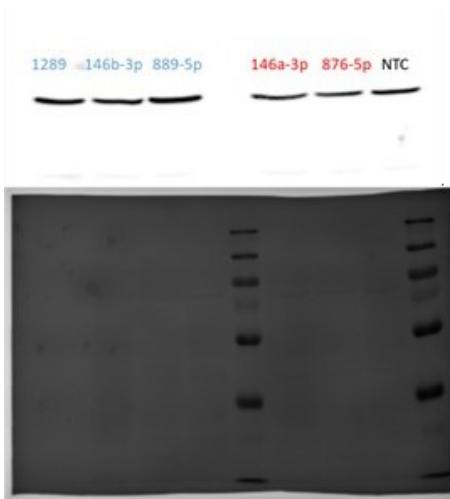
<b>miRNA</b>	<b>Normalization over NTC</b>	<b>Z-score</b>
hsa-miR-876-5p	0.38098	-2.35311
hsa-let-7g-5p	0.609172	-1.60088
hsa-miR-3921	0.643201	-1.48871
hsa-miR-661	1.548614	1.495945
hsa-miR-1289	1.56616	1.553784
hsa-miR-146b-3p	1.839292	2.454152
hsa-miR-212-5p	1.917496	2.711947
hsa-miR-129-1-3p	1.930105	2.753514
hsa-miR-124-3p	2.071235	3.218743
hsa-miR-1254	2.087368	3.271923
hsa-miR-3135b	2.329111	4.068821
hsa-miR-889-5p	2.43549	4.419493
hsa-miR-92a-1-5p	4.674151	11.79915
hsa-miR-4434	0.404793	-2.27461
hsa-miR-4460	0.543127	-1.8186
hsa-miR-4709-3p	0.556351	-1.77501
hsa-miR-6875-3p	0.562321	-1.75533
hsa-miR-5100	0.595801	-1.64496
hsa-miR-1269a	0.605405	-1.6133
hsa-miR-4536-5p	0.631214	-1.52822
hsa-miR-432-3p	0.635394	-1.51445
hsa-miR-125a-5p	0.636496	-1.51081
hsa-miR-4764-5p	0.63942	-1.50117
hsa-miR-122-5p	0.654305	-1.45211
hsa-miR-3691-5p	0.656438	-1.44508
hsa-miR-6832-3p	1.532196	1.441822
hsa-miR-1238-3p	1.532811	1.44385
hsa-miR-223-5p	1.535026	1.451151
hsa-miR-361-5p	1.537228	1.458412
hsa-miR-1256	1.539574	1.466145
hsa-miR-1306-3p	1.54531	1.485052
hsa-miR-3679-3p	1.54669	1.489603
hsa-miR-548ae-3p	1.547477	1.492196
hsa-miR-877-5p	1.549	1.497216
hsa-miR-4649-5p	1.551428	1.505222
hsa-miR-4722-3p	1.552085	1.507385
hsa-miR-342-5p	1.55333	1.511492
hsa-miR-630	1.558231	1.527647
hsa-miR-766-3p	1.560197	1.534126
hsa-miR-767-5p	1.562354	1.541238
hsa-miR-574-5p	1.563649	1.545508
hsa-miR-329-5p	1.565202	1.550626

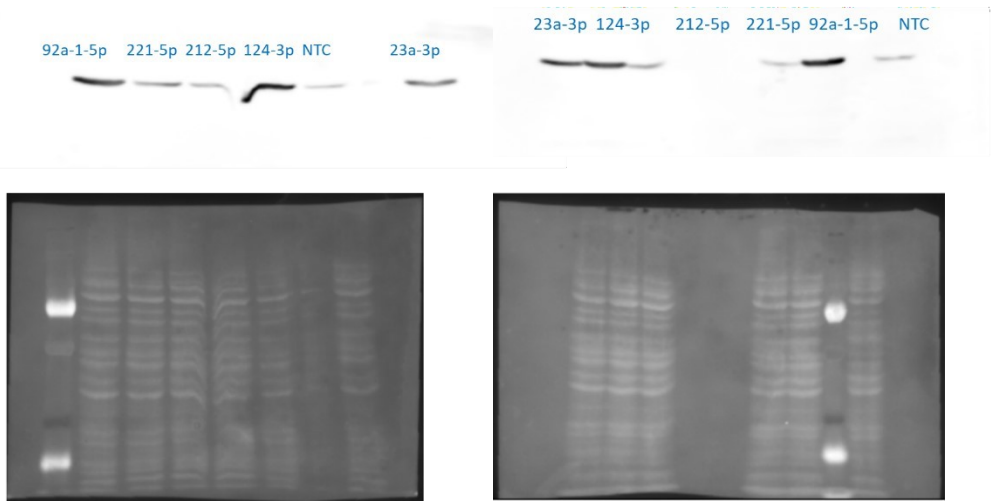
hsa-miR-617	1.566998	1.556545
hsa-miR-3186-3p	1.567691	1.558831
hsa-miR-361-3p	1.569855	1.565963
hsa-miR-597-5p	1.573642	1.578448
hsa-miR-574-3p	1.576869	1.589085
hsa-miR-1228-3p	1.579112	1.596481
hsa-miR-6789-5p	1.581066	1.602921
hsa-miR-663b	1.587861	1.625321
hsa-miR-8081	1.591082	1.635939
hsa-miR-6504-5p	1.595132	1.649289
hsa-miR-5092	1.596288	1.6531
hsa-miR-200b-5p	1.596898	1.655109
hsa-miR-3163	1.602341	1.673055
hsa-miR-4650-5p	1.602686	1.67419
hsa-miR-548h-3p	1.612655	1.707053
hsa-miR-4268	1.613386	1.709463
hsa-miR-132-5p	1.623876	1.744043
hsa-miR-4732-3p	1.630792	1.76684
hsa-miR-4693-5p	1.636494	1.785638
hsa-miR-6502-3p	1.637094	1.787616
hsa-miR-6076	1.639407	1.79524
hsa-miR-4652-5p	1.640143	1.797665
hsa-miR-6744-3p	1.651578	1.835362
hsa-miR-4707-5p	1.65813	1.85696
hsa-miR-4740-3p	1.669992	1.896061
hsa-miR-5010-3p	1.672801	1.905323
hsa-miR-219b-5p	1.677102	1.9195
hsa-miR-5193	1.677279	1.920085
hsa-miR-5590-3p	1.688818	1.95812
hsa-miR-3154	1.691382	1.966573
hsa-miR-4667-5p	1.691633	1.967399
hsa-miR-151b	1.692238	1.969397
hsa-miR-3176	1.702083	2.00185
hsa-miR-6886-5p	1.708752	2.023832
hsa-miR-421	1.709957	2.027806
hsa-miR-4435	1.720565	2.062775
hsa-miR-4778-5p	1.727564	2.085846
hsa-miR-5702	1.732885	2.103387
hsa-miR-6723-5p	1.746261	2.14748
hsa-miR-4690-5p	1.751317	2.164148
hsa-miR-135b-3p	1.756436	2.181022
hsa-miR-1231	1.767392	2.217138
hsa-miR-4754	1.772049	2.232488
hsa-miR-18b-3p	1.784172	2.272453
hsa-miR-3181	1.787377	2.283018

hsa-miR-4749-5p	1.790093	2.291969
hsa-miR-6855-5p	1.797519	2.316448
hsa-miR-3128	1.802085	2.331501
hsa-miR-4800-3p	1.803963	2.337693
hsa-miR-4666b	1.816292	2.378334
hsa-miR-6850-5p	1.840217	2.457201
hsa-miR-4725-5p	1.853643	2.501459
hsa-miR-4795-5p	1.866374	2.543426
hsa-miR-3926	1.879387	2.586322
hsa-miR-4785	1.886119	2.608515
hsa-miR-4749-3p	1.89837	2.648901
hsa-miR-7-2-3p	1.90384	2.666932
hsa-miR-4747-3p	1.914069	2.70065
hsa-miR-4467	1.915511	2.705404
hsa-miR-4697-3p	1.920371	2.721427
hsa-miR-488-5p	1.923402	2.731419
hsa-miR-5685	1.927115	2.743658
hsa-miR-372-3p	1.942605	2.794718
hsa-miR-1226-5p	1.95357	2.830864
hsa-miR-4789-5p	1.98895	2.947494
hsa-miR-23b-5p	1.989137	2.948112
hsa-miR-3922-5p	2.012974	3.026689
hsa-miR-4707-3p	2.019163	3.04709
hsa-miR-548au-5p	2.039283	3.113415
hsa-miR-449b-5p	2.054087	3.162216
hsa-miR-634	2.084458	3.262332
hsa-miR-3193	2.093941	3.293592
hsa-miR-3184-5p	2.157327	3.50254
hsa-miR-3192-5p	2.185694	3.596053
hsa-miR-4255	2.199637	3.642014
hsa-miR-1180-3p	2.235002	3.758595
hsa-miR-4524a-3p	2.235838	3.76135
hsa-miR-4720-5p	2.305796	3.991964
hsa-miR-506-3p	2.648716	5.122384
hsa-miR-30c-1-3p	2.663032	5.169577
hsa-miR-196a-3p	2.736287	5.411058
hsa-miR-4470	3.290954	7.239495
hsa-miR-3123	3.377701	7.525455

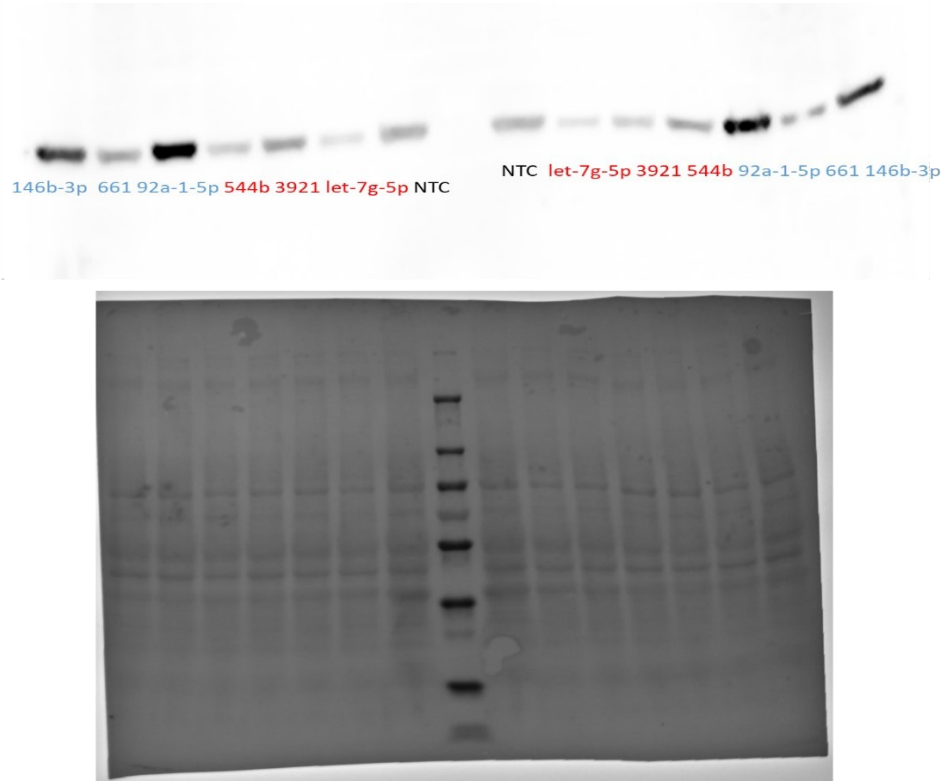
## Appendix-6: Ponceau images of Western blots in HT29







**Appendix-7: Ponceau images of Western blots in A549**





**Appendix-8: Ponceau images of Western Blots in PANC1:**

